2016

Impact of the Charge-Regulation Effect on Bacterial Growth and Bioavailability of Sorbed Growth Substrates

Hankai Zhu
Lehigh University

Impact of the Charge-Regulation Effect on Bacterial Growth and Bioavailability of Sorbed Growth Substrates

by

Hankai Zhu

A Dissertation

Presented to the Graduate and Research Committee

of Lehigh University

in Candidacy for the Degree of

Doctor of Philosophy

in

Environmental Engineering

Lehigh University

(May, 2016)

Approved and recommended for acceptance as a dissertation in partial fulfillment of the requirements for the degree of Doctor of Philosophy.

_____

Date

_____

Prof. Derick G. Brown

Dissertation Director

Civil and Environmental Engineering

_____

Accepted Date

Committee Members:

_____

Prof. Arup K. SenGupta

Dissertation Committee Chairperson

Civil and Environmental Engineering

_____

Prof. Kristen Jellison

Civil and Environmental Engineering

_____

Prof. Muhannad Suleiman

Civil and Environmental Engineering

_____

Prof. Bryan W. Berger

Chemical and Biomolecular Engineering

Acknowledgments

This study was partially funded by the National Science Foundation through Grant 0828356; a grant from Evoqua Water Technologies, LLC; and the Pennsylvania Department of Community and Economic Development through Pennsylvania Infrastructure Technology Alliance (PITA) and Research for Advanced Manufacturing in Pennsylvania (RAMP) grants. The author gratefully acknowledges their valuable support during this work.

Table of Contents

List of Tables

List of Figures

Abstract

Bacteria are typically found attached to surfaces. Their growth on surfaces can be beneficial, such as with trickling filters, bio-filters and bio-scrubbers, where the attached bacteria are used to biodegrade aqueous organic components. There are also plenty of systems where bacterial surface growth is not desirable, such as with biofilm formation in water distribution pipelines and pathogenic biofilm infections on medical implants and equipment. One consideration in all these systems is the interaction between the bacteria and the adhering surface, and specifically, how the physiochemical properties of the surface can influence bacterial growth.

Previous studies demonstrated that the metabolic activity of bacteria could be altered upon adhesion onto solid surfaces. The underlying mechanism remained unclear until the theory linking the charge-regulation effect to cellular bioenergetics was developed by Hong and Brown. Surfaces in the aqueous environment are typically charged due to ionization of acidic (negatively-charged) and basic (positively-charged) functional groups at the surface. These “charge-regulated” surfaces exhibit surface charge and electrostatic potential variation as a function of pH. When charge-regulated surfaces approach each other, such as when a bacterium approaches a solid surface, the surface charge and electrostatic potential will vary as a function of separation distance. This in turn causes the local pH to vary, following the Boltzmann distribution, and this will alter the surface functional group ionization, which affects the surface charge. The end results of these complex interactions is that the surface charge, electrostatic potential and pH will all vary

as a function of separation distance between the surfaces. This is the so-called charge-regulation effect and it can be modeled as a function of the dissociation constants and site density of the surface functional groups.

This study is based on the hypothesis linking cellular bioenergetics, where energy is stored as proton gradient across the bacterial cytoplasmic membrane, and the charge-regulation effect, where the cell surface proton concentration is altered during adhesion. Previous studies have shown that bioenergetics is affected by the charge-regulation process and that the effect is a direct function of the acidic and basic functional groups on the adhering surface. These studies were performed under non-growth conditions, and demonstrate that activity increases for acidic surfaces and decreases for basic surface, in agreement with the hypothesis. The purpose of this study was to build upon the prior studies and examine how charge-regulated surfaces can affect the growth of bacteria.

First, we developed and demonstrated a simple approach for characterizing charge-regulated surfaces using zeta potential – pH titration data. The purpose was to model the surface electrostatic potential and charge density as a function of pH. This allowed modeling of the materials used in this study and interpretation of the experimental results. Having knowledge of surface properties, preliminary biodegradation experiments were conducted using regular sand (acidic functionality) and iron-coated sand (basic functionality). The results demonstrated that attached bacterial growth was directly affected by the charge-regulation effect. The iron-coated sand carrying more positive

charge at the surface exhibited antimicrobial properties as compared to the uncoated sand, which is in agreement with our working hypothesis for charge-regulated surfaces.

We then focused on three different granular activated carbon (GAC) materials, all provided from Evoqua Water Technologies, LLC. These included an untreated GAC, a GAC that was modified to contain a surface-bound weak base, and a GAC that was modified to contain a surface-bound strong. Surface analysis demonstrated that the untreated GAC was negatively-charged, whereas the treated GACs exhibited increased positive charge from the weak-base to the strong-base. Enhanced nitrogen content due to the applied bases on the treated GAC surfaces was confirmed with SEM/XRD.

Using the three GACs, we performed biodegradation (respirometry) experiments using benzoic acid as the growth substrate. At higher concentrations of benzoic acid, bacterial growth was reduced in the presence of the treated GACS, with the effect more pronounced with the strong-base GAC, as expected following the hypothesis. At a low concentration of benzoic acid, however, we saw the exact opposite results, and let to a new and unexpected research finding, related to how the charge-regulation effect can alter the sorption – and thus bioavailability – of ionizable growth substrates.

We explored this using three different growth substrates – benzoic acid (weak acid), benzylamine (weak base), and ethylbenzene (neutral). Using these growth substrates, we examined their sorption and bioavailability with each GAC. Substrate sorption isotherm on the GACs was strongly affected by surface pH, and this strongly affected the

bioavailability of the different growth substrates via charge-regulated variations in local pH. For example, the modeling results indicated an increase in local pH upon bacterial adhesion onto strong-base GAC, which carried more positive charges. The sorption of benzoic acid decreases with increasing pH, and this resulted in release of sorbed benzoic acid and an increase in the aqueous concentration available for bacterial growth.

This study has demonstrated that the charge-regulation effect can impact both bacterial activity (via changes in cellular bioenergetics, which is dependent on a pH gradient across the cell membrane) and bioavailability of sorbed, ionizable growth substrates (via changes in the substrate ionization). The overall relationship between surface electrostatic properties and cellular bioenergetics provides were demonstrated through experimentation and modeling using the charge-regulation model. Understanding of this effect can allow more effective selection and specific design of surfaces given the goals of the specific system.

CHAPTER 1

INTRODUCTION AND OVERVIEW

CHAPTER 1 Introduction and Overview

1.1 Introduction and Background

Bacteria are typically attached to and growing upon sorts of surfaces in natural environment. Microbial adhesion to interfaces and following reactions serves or hinders multiple engineering applications. In some cases, bacterial attached growth is highly desirable, such as the application of organic contaminant removal process and attached growth bioreactors can benefit from biofilm growth (Carol *et al*., 1994; Bowera *et al*., 1996). On the other hand, in many other environments, bacterial adhesion and biofilm formation are detrimental such as pathogenic infections on medical equipment, biofilm formation in water distribution pipelines and food-contact surfaces (Gibbons, 1984; Buonocore *et al*., 1956). The selection of appropriate solids and optimization of environmentally benign materials are vital for bioreactor design and bioremediation process.

The interaction between the bacteria and the adhering surface, and specifically, how the physiochemical properties of the surface can influence bacterial growth has been proposed, and then explored and demonstrated by the following researchers. Once bacterial metabolic activity levels are enhanced or declined, it can control more over the microbial colonization process. Zobell (1943) was the first to report an increase in the ability of bacteria attached to the walls of glass flasks. Microbial adhesion and other

related processes such as bacterial transport through porous media and biofilm formation, are also highly influenced by the electrostatic nature of the solid surfaces. Based on those early observations, researchers examined a range of materials for that effect on bacterial activity, including glass; polymers such as polystyrene, Teflon, polyethylene; resin beads with amino groups and silver used in our current experiment (Mafu *et al*., 2011; Terada *et al*., 2006; Schie and Fletcher, 1999).

Numerous trials have been done to explore the general influence of bacterial adhesion on biological process in environmental remediation. They focused the response of cells upon approaching different solid surfaces, and revealed that the surface attachment would affect cellular metabolic activity level (Petersen and Moller, 2000). However, the explanation of why microbial adhesion affects cellular activities and how the surface charge distribution varies when a cell approaches or attaches solid surfaces is controversial and lack of theoretical verification. Hong and Brown (2009) proposed a link between the physiochemical charge-regulation effect, which occurs as a surface possessing acid/base functional groups approaches another surface, and cellular bioenergetics, where adenosine triphosphate (ATP) is produced from the proton motive force (Δp) and drives cellular growth (Figure 1.1). The previous work in our lab demonstrated that the bioenergetics of adhered bacterial cells varied depending on the specific electrostatic nature of attached surfaces under non-growth condition. Here, this study further examined *Pseudomonas putida* cells with growth to determine how the microbial growth rate would be affected by the physiochemical properties of adhered

surfaces. Our working hypothesis relates the surfaces nature to bacterial metabolic activity and growth kinetics.

Besides organic compound adsorption to charged interfaces has an increasing attention throughout natural sciences and environmental remediation issues (Ravichandran and Talbot, 2000; Gong and Szleifer, 2004). Previous findings described how bulk pH and ionic strength altered the equilibrium adsorption of ionizable compounds (Al-Degs *et al*., 2008; Biesheuvel *et al*., 2005). Subsequent studies tried to explain such a shift in adsorption capability through free energy analysis, Van der Waals dispersion forces, and electrostatic interactions among small ions, surface and electrolyte (Czeslik and Winter, 2001). Despite the electrostatic and chemical processes of adsorption to the charged interfaces have been well studied, few reports showed the direct link between microorganism adhesion to surfaces with specific electrostatic nature and compound sorption condition. It remains unclear about how to connect surface electrostatic properties to microbial attached growth via both bioavailability and bioenergetics.

This study incorporated cellular bioenergetics, surfaces physicochemical properties and substrate sorption isotherm examination to develop the charge-regulation model when two surfaces with acid/base functional groups approach each other. Our proposed hypothesis of charge-regulation effect about bioenergetics showed a consistent result with the study completed by other groups (Hong and Brown, 2009). While, the charge-regulated surfaces were demonstrated to govern the biodegradation process for those

environmental system associated with activated carbon, which in turn directly affected microbial growth under substrate limit condition. This work would help understand the coupled influence of bacterial adhesion and variation in local pH on both cell surface and solid surfaces considering bioenergetics and sorption condition.

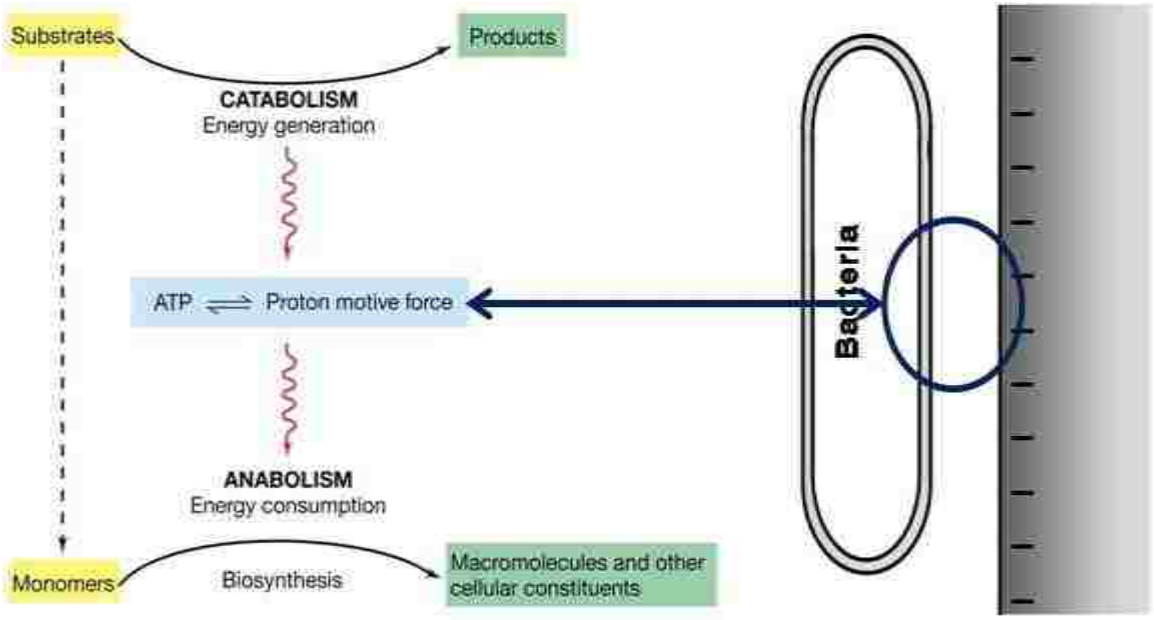

Figure 1.1 - The figure depicts cellular bioenergetics and metabolism within the cell upon adhesion. The energy generation and consumption processes of microorganisms occur inside the cell coupling with microbial catabolism and anabolism, respectively. The energy released from catabolic process is captured to produce ATP from ADP, and is potentially used to drive anabolic process to produce cellular components. The working hypothesis suggest a link between cellular bioenergetics and the physiochemical charge-regulation effect, which occurs as a surface with acid/base functional groups the bacterial cell surface) approaches another surface.

1.2 Cellular Bioenergetics and Microbial Growth

The working hypothesis is based on a link between the charge-regulation effect, which occurs at the bacterial cell surface, and cellular bioenergetics, where bacteria obtain energy from catabolic processes. Cellular bioenergetics describes the catabolic process (where reactions occur to provide energy) and anabolic process (where reactions occur to utilize energy to maintain the cell or support microbial activities). Figure 1.3 shows briefly how energy is obtained from electron-rich substrates. In this process, electrons are passed from the electron donor (i.e., the energy substrate being consumed by the bacteria) down through an electron transport chain and ultimately to the terminal electron acceptor (e.g., oxygen). During respiration (catabolic reactions) where the electrons are being passed through the electron transport chain, protons are pumped out of the cytoplasmic membrane, creating both a pH and a charge gradient across the membrane. This electrochemical gradient composed of both pH and electrostatic potential gradients is termed the proton motive force (Δp), which can be expressed as

$$\Delta p = \Delta\psi - 2.303\frac{RT}{F}\Delta pH \quad (1)$$

where Δp is the proton motive force (mV), ΔΨ is the membrane electrostatic potential (mV), ΔpH is the pH gradient across the cell membrane, F is the Faraday constant, R is the universal gas constant and T is the temperature. At 25 ℃ it can be written as

$$\Delta p = \Delta\psi - 60\Delta pH \quad (2)$$

Both gradients are built up during oxidative phosphorylation. Considering neutrophilic bacteria $\Delta\psi$ typically contributes 70-80% of the Δp and ΔpH accounts for 20-30% (White, 2000).

The energy stored in proton motive force (Δp) is used to produce adenosine triphosphate (ATP), where the protons are allowed to reenter the cell via the reversible enzyme ATP synthase and ATP is formed from phosphate and adenosine diphosphate (ADP). This is a reversible thermodynamic process and Δp is related to the phosphorylation potential as (Jones, 1988).

$$Fn\Delta p = \Delta G_p = \Delta G_p^{\circ\prime} + 2.303RTlog\left(\frac{[ATP]}{[ADP][P_i]}\right) \qquad (3)$$

where ΔG_p is the phosphorylation potential; ΔG_p° is the standard free energy for ATP hydrolysis; n is the number of protons translocated by the ATP synthesis enzyme per ATP synthesized; and [ATP], [ADP], and [P_i] are the cellular concentrations of ATP, ADP, and phosphate, respectively. Thus, if Δp increases, then ATP increases. Otherwise, ATP should decline with decreased Δp. The formation of ATP and Δp are described as processes A, B and C in Figure 1.2. A change in ATP or Δp formation in the cell should directly link to variation of the overall metabolic activity (Madigan *et al*., 2000).

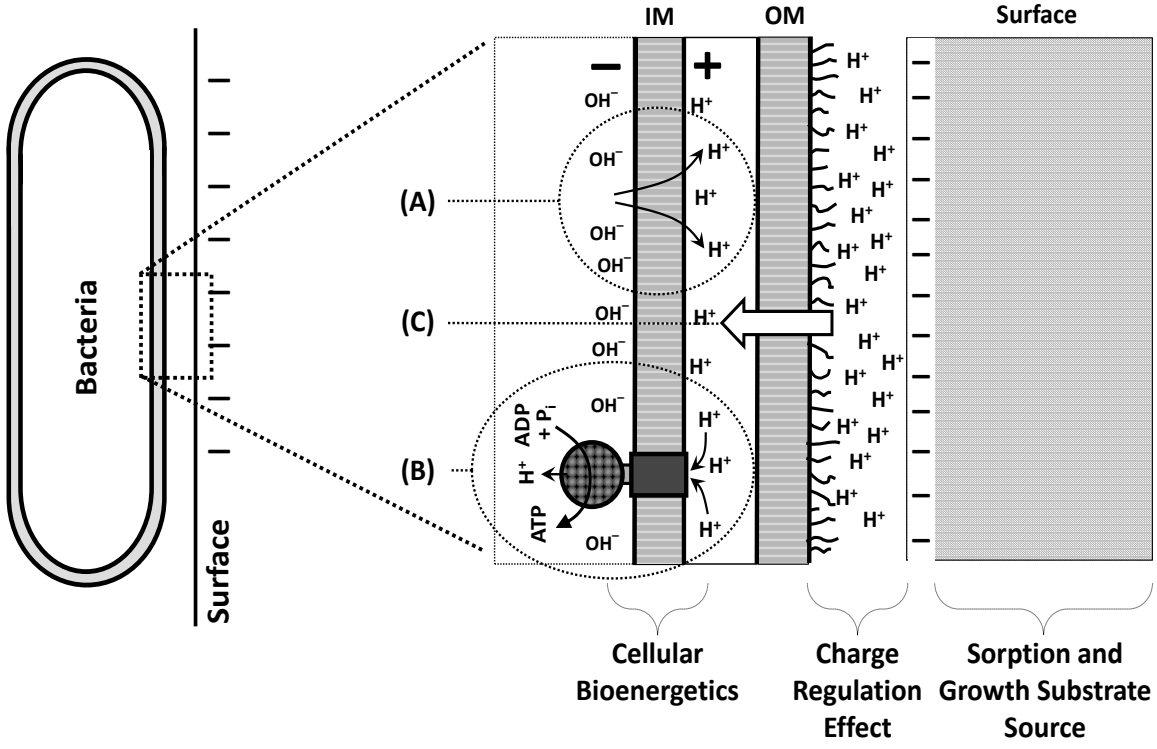

Figure 1.2 - The presented hypothesis about the charge-regulation effect on cellular bioenergetics described here a Gram-negative bacteria cell approaching a negatively-charged solid surface. During process A, protons are being pumped across the inner (cytoplasmic) membrane (IM) during respiration, Energy is stored in the resulting proton gradient across the cell membrane and it is quantified as the proton motive force (Δp). This Δp is then used to create ATP from ADP when the protons are allowed back across the IM as depicted in process B. Process C indicated that any variation of proton concentration at the charge-regulated surface upon approaching should pass the outer membrane (OM) and affect the proton gradient. The ATP level and microbial activity would be accordingly altered.

1.3 The Charge-Regulation Effect

Charged surfaces are present everywhere, and numerical natural phenomena and man-made processes are governed by electrostatic behavior and interactions between the charged surfaces. Electrostatic interaction played a vital role in determining the physical and chemical behavior of solutions in the vicinity of interfaces, where the charge-regulated surfaces result from the ion distribution on the approaching surfaces. The interaction involves the dissociation of surface ionic groups and the attraction towards ions from bulk. The electrostatic potential within nano-scale distance between interfaces as well as proton distribution would be directly affect such interaction of an interface with an adjacent polar liquid (e.g. salty water). It is important to study into the influence of electrostatic behavior associated with local pH on electrokinetic transport in fluidic channels and throughout microorganism membrane, which induces a shift in cellular bioenergetics in Figure 1.3.

This work was to determine whether or not the charge-regulation effect upon microbial adhesion induces the variation of proton concentration at the cell surface, and thus affect microbial activities. The charge-regulation model was proposed and applied to the bacterial adhesion process in conjunction with the analysis on surface physicochemical properties of both bacteria and solid materials.

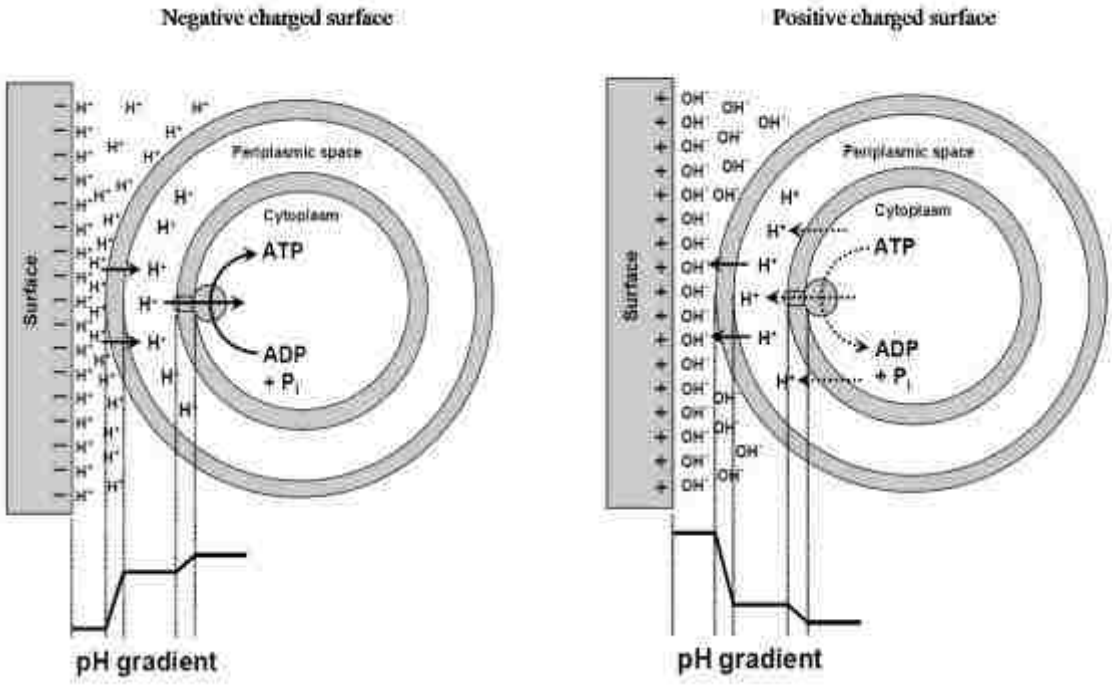

Figure 1.3 - Proposed hypothesis for a gram-negative bacterial cell approaching to negatively and positively charged surfaces (Yong and Brown, 2009). The charge regulation effect results in an increase and decline in local proton concentration between the cell and the negatively charged surface and positively charged surface, respectively. The changes in proton concentration vary responding to Δp, which determines ATP level in the cell and cellular growth kinetics.

1.3.1 The Charge-Regulation Model

When a charged surface approaches another surface, counter ions tend to assemble at the surface to maintain the nature of neutrality. The competition between counterion neutralization and the rapid thermal molecular motion creates an electric double layer. The distribution of counter ions adjacent to a charged surface can be calculated. The charge-regulation model proposed here was simulated based on solving the Poisson–Boltzmann equation with charge regulation boundary conditions that account for the surface-aqueous solution chemical equilibrium. The model describes the electrostatic potential in an electrolyte solution as a function of distance from a charged surface. The charge-regulation boundary conditions were first formulated by Ninham and Parsegian (Ninham and Parsegian, 1971), and follows the model presented here was developed in Hong and Brown (Hong and Brown, 2008; Hong and Brown, 2010), considering the multiple functional groups on adhering surfaces. The charge-regulation model describes electrostatic potential in an electrolyte solution as a function of distance from a charged surface. In one-dimension it is written as

$$\frac{d^2\psi}{dx^2} = -\frac{1}{\varepsilon_0 \varepsilon}\sum_i n_{ri}\, z_i e exp\left(\frac{-z_i e\psi}{kT}\right) \tag{3}$$

where x is the distance from the charged surface; $\boldsymbol{\psi}$ is the electrostatic potential (V); ε_0 is the permittivity of vacuum (8.854×10^{-12} C^2/J-m); ε is the dielectric constant of the medium (78.5 for water); n_{ri} is the number of ions of species i per unit volume in the bulk fluid; z_i is the valence of ion i; e is the electron charge (1.602×10^{-19} C); k is the

Boltzmann constant (1.381×10^{-23} J/K); and T is the temperature (K). Gauss's law is applied to provide the boundary conditions to Equation 3 and it can be written as

$$\frac{d\psi}{dx}\Big|_i = -\frac{1}{\varepsilon_0 \varepsilon}\sigma_i \tag{4}$$

Where σ is the surface charge density (C/m^2) and subscript i defines the two surfaces. The basis of the charge-regulation effect is that the charges at the two surfaces in Equation 4 are controlled by the dissociation of the acid/base functional groups:

$$R_{aj}H \leftrightarrow R_{aj}^{-} + H^{+} \tag{5}$$

$$R_{bk}H^{+} \leftrightarrow R_{bk} + H^{+} \tag{6}$$

Where R_{aj} are the acidic ionizable sites of type j (e.g., phosphoric, carboxylic and hydroxyl groups) and R_{bk} are the basic ionizable sites of type k (e.g., amine groups). The dissociation constants associated with these surface functional groups (K_{aj} and K_{bk}) are

$$K_{aj} = \frac{\left[R_{aj}^{-}\right]\left[H^{+}\right]_s}{\left[R_{aj}H\right]} \tag{3}$$

$$K_{bk} = \frac{\left[R_{bk}\right]\left[H^{+}\right]_s}{\left[R_{bk}H^{+}\right]} \tag{4}$$

where $[R_x]$ and $[R_xH]$ are the areal densities (molecules per unit surface area) of the dissociated and associated functional groups and $[H^+]_s$ is the molar concentration of hydrogen ions near the surface. $[H^+]_s$ is calculated using the Boltzmann distribution,

$$[H^+]_s = [H^+]\exp\left(-\frac{e\psi_s}{kT}\right) \quad (5)$$

where $[H^+]$ is the molar concentration of hydrogen ions in the bulk solution; ψ_s is the surface electrostatic potential (V).

Referring the calculation of dissociation constants associated with these functional groups on surface i, the charge density of surface i is considered as that the total number of positively charged sites minus that of negatively charged sites.

$$\frac{\sigma_i}{e} = \sum_k [R_{bki} H^+] - \sum_j \left[R^-_{aji}\right] \quad (7)$$

By combining these equations, an expression for the surface charge density was addressed as a function of the dissociation of the acid/base functional groups:

$$\frac{\sigma_i}{e} = \sum_k \left[\frac{[H^+]N_{bki}}{[H^+]+K_{bki}\,exp\left(e\Psi_{si}/(kT)\right)}\right] - \sum_j \left[\frac{K_{aji}\,N_{aji}}{K_{aji}+[H^+]exp\left(-e\Psi_{si}/(kT)\right)}\right] \quad (8)$$

where N_{aji} and N_{bki} are defined as the number of acid sites of type j and base sites of type k per unit area of surface i; K_{aji} and K_{bki} are defined as the dissociation constants associated with these functional groups on surface i.

In these equations, the surface acid/base properties are represented in terms of N_{aji}, K_{aji}, N_{bki} and K_{bki}. With bacteria, the surface charge arises via the dissociation of carboxylic, phosphoric, hydroxyl, and amine groups (Hong and Brown, 2006; Atrih *et al*., 1999; Beveridge, 1981). These functional groups are associated with peptidoglycan, teichoic, and teichuronic acids on the surface of gram-positive bacteria and with

lipopolysaccharides, phospholipids, and proteins on the surface of Gram-negative bacteria. Thus, with knowledge of the surface acid/base properties, Equations 3 and 8 allow calculation of the electrostatic potential profile between the bacterial and solid surfaces. The local pH is then calculated via application of the Boltzmann distribution.

Bioenergetics is based on a pH and charge gradient across the cytoplasmic membrane. The hypothesis indicates that when cells approach solid surface, the change in cell surface electrostatic potential and pH, which results from the charge-regulation effect, will in turn affect Δp, with a corresponding change in cellular ATP levels. The working hypothesis indicates that changes in pH and ψ at the cell surface will affect the pH and ψ gradients across the cytoplasmic membrane, and thus affect cellular bioenergetics. This is depicted in Figure 1.3, where we hypothesized that when cells approach a negatively (or positively) charged surface, the local pH at the cell surface will decrease (or increase), which in turn enhances (or reduces) the proton gradient across the cell membrane and ultimately ATP formation.

Experimental evidence to date supports this hypothesis. Previous research in our laboratory with stationary-phase bacteria demonstrated a rapid enhancement in cellular ATP levels when bacteria adhered onto glass surfaces and example results are shown in Figure 1.4 (Hong and Brown, 2009). And ongoing research with stationary-phase bacteria is demonstrating that adhesion to positively-charged surfaces containing amine functional groups results in a decrease in bacterial ATP levels. These studies all support the

hypothesis that bacterial metabolic activity is strongly influenced by a link between cellular bioenergetics and the physiochemical charge regulation effect as a surface approaches another surface.

1.3.2 The Charge-Regulated Surfaces

The properties of solid/liquid interfaces have direct influence on multiple environmental processes of adsorption, filtration or separation. Consequently, environmentally benign materials with multifunctional surfaces obtained from proper surface modification are desirable nowadays in a variety of application, such as biodegradation and site cleanup remedies.

Bacterial cell membrane consists of lip bilayers, the cell wall, glycocalyx, and intracellular cytoskeleton. The microorganism cell surfaces are generally associated with both acidic and basic functional groups including hydroxyl, carboxyl, phosphoryl, and amide groups. The cell polarity is generally characterized by the electrophoretic mobility of cells in an electric region. Typically, bacterial cells possess net negative electrostatic charge due to ionized phosphoryl and carboxylate substituents on outer cell envelope macromolecules in most environments. Gram positive bacteria exhibit negatively charged surface due to the presence of teichoic acids, which is negatively charged, linked to either the peptidoglycan or to the underlying plasma membrane; the Gram negative bacteria have an outer membrane containing phospholipids and Lipopolysaccharides, which allow the cell surfaces carrying a strong negative charge.

The working model is capable of representing charge-regulated surfaces, including both solid surface and bacterial cell surface as in Figure 1.5 for example (Yong and Brown, 2008). When the bacterial cell approaches another surface, the surface electrostatic potential and pH of the cell will be altered by the charge-regulation effect. Our hypothesis links the physicochemical nature of surfaces to the cell surface pH, and accordingly the cellular ATP concentration and microbial activities.

This study is addressed by applying the charge-regulation model to the bacteria/solids system. The Poisson distribution of ions as point charges at the surface is assumed. The surface charge is determined by the extent of the surface ionization and binding reactions, both of which should be affected when being exposed to specific local ionic environment. We characterized both bacterial cells and material solid surfaces throughout a combination of electrophoretic mobility measurements and potentiometric titration. The potentiometric titration governs the acid/base properties of the surfaces, and the values of pK and N could accurately describe the physicochemical nature of surfaces. Understanding the properties of bacterium/solid and solid/liquid interfaces is vital for designing surface-modified materials for specific issues.

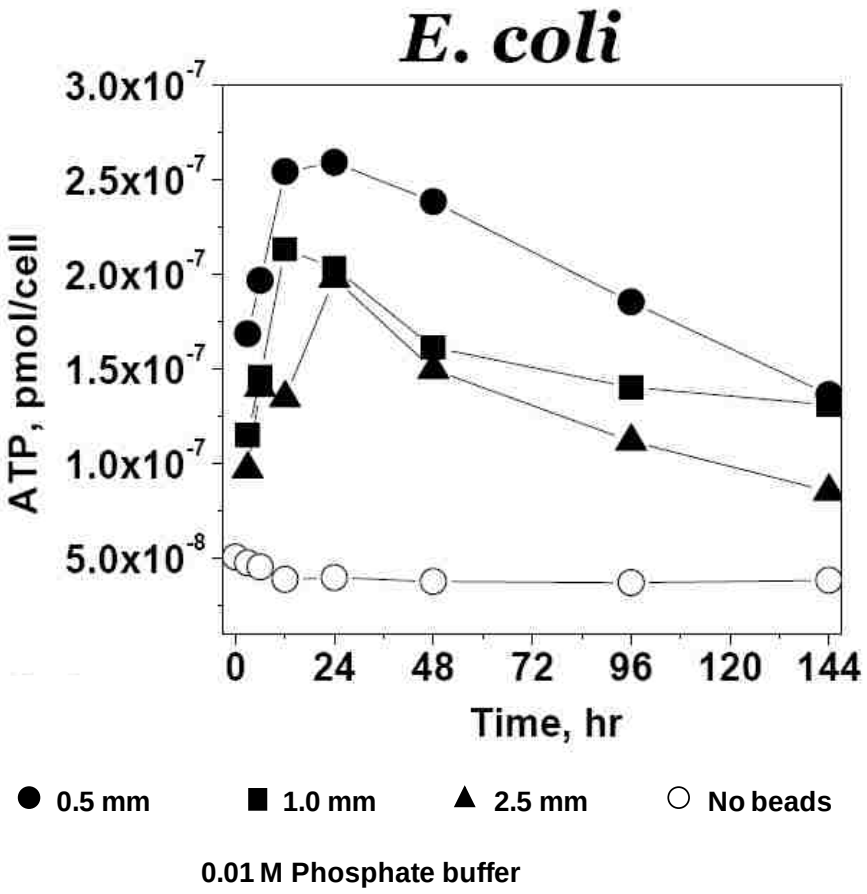

Figure 1.4 - Example result of adenosine triphosphate (ATP) response upon microbial adhesion of *E. coli* (Hong and Brown, 2009). ATP levels involving cell numbers for planktonic cells and adhered cells on 0.5-mm, 1.0-mm, and 2.5-mm glass beads. A significantly enhancement in cellular metabolic activity (represented as ATP level) were obversed to occur when adhering to glass beads.

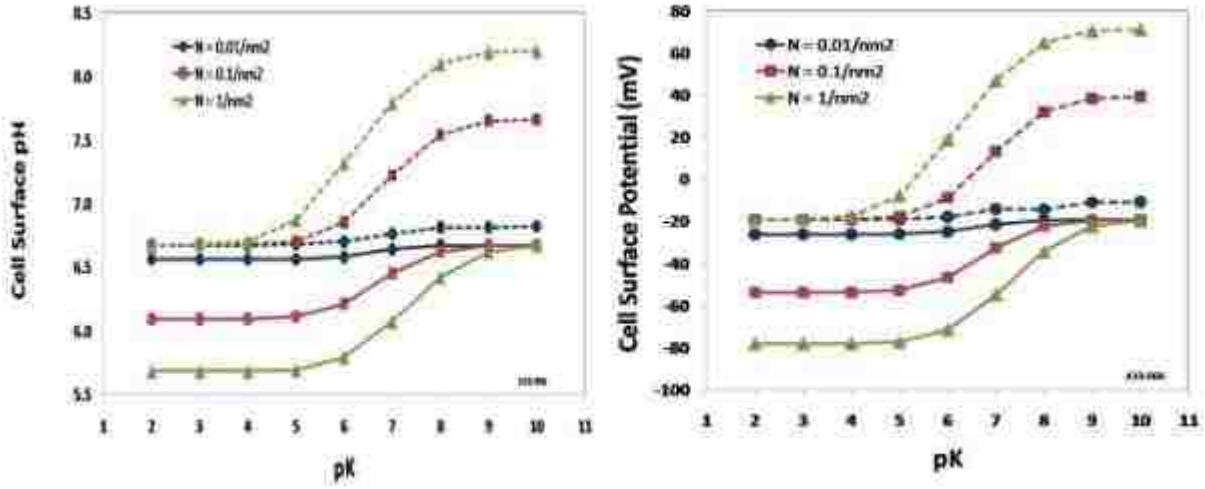

Figure 1.5 - Samples of charge-regulation modeling results for *E. coli* K-12. This figure indicates the surface pH and electrostatic potential of an cell attached to a solid surface containing a single type of acid/base functional group. The solid surface is represented by the dissociation constant (pK) and the area site density (N) of the functional group on the solid surface, along with whether the functional group is negatively-charged (solid lines, e.g., carboxyl group) or positively-charged (dashed lines, e.g., amine group). The results were predicted using the charge-regulation code and measured surface properties of *E. coli* K-12, and the symbols represent individual model runs.

1.4 Project Goals and Objectives

The working hypothesis describes how the adhesion can affect celluar ATP levels and microbial activities, based on a link between the physicochemical charge-regulation effect, which results in a change in electrostatic potential and pH at the bacterial cell surface as the cell approaches another surface, and cellular bioenergetics and microbial growth, which is based on electrostatic potential and pH gradients across the bacterial cytoplasmic membrane (Hong and Brown, 2006; Hong and Brown, 2008; Hong and Brown, 2009; Hong and Brown, 2010). The hypothesis indicates that changes in the electrostatic potential and local pH at the cell surface will affect the gradients across the cytoplasmic membrane and ultimate result in changes in cellular bioenergetics. Current research with stationary-phase bacterial cells (i.e., the cells are not growing) has supported this hypothesis. This study will focus on cells undergoing active growth to determine if the growth of attached bacteria is influenced by the solid surface as predicted by the working hypothesis. Both enhanced biodegradation and inhibited bacterial growth upon adhering to specific charged surfaces were observed and explained in the framework of charge regulation theory in the following chapters.

1.4.1 Objective 1: Develop an Approach to Characterize and Quantify the Charge Regulated Surfaces.

Adhering to solid surfaces can directly influence cellular response, and ultimately microbial activities. Characterization of material surfaces in terms of the dissociation

constant (K) and charge density (N) of each functional group is desirable in multiple environmental processes (Sheng *et al*., 2010). Here we develop a mathematic method for quantifying the functional groups with Ka and Na using parameter estimation code PEST (Watermark Numerical Computing), which was developed in C++ to estimate and optimize the charge-regulation process. Rather than identifying an specific Ka and Na, our goal is to represent an appropriate electrostatic nature of surfaces in specific electrolyte solution. The approach about how to optimize modeling parameters is elucidated, and the modeling results are verified by running with different electrolyte concentrations. This work allows the quantification the surface physicochemical properties, and provides a feasible way to select appropriate material for specific application.

1.4.2 Objective 2: Apply Our Hypothesis of Charge-Regulation about Bioenergetics to Microbial Growth Experiments with Surface Characterization

The approach here is to apply charge-regulation model to different materials, including *P. putida* cells, untreated, weak base- and strong base-treated activated carbons (GACs) as well as regular silica sand and iron coated sand. The zeta potential profile with pH from electrophoretic mobility measurements was used to model the electrostatic behavior of approaching surfaces using Poisson-Boltzmann equation as developed in Objective 1. We demonstrated that both base treatment on activated carbon and iron coating with sand did add more positive charge at the surfaces. The surface charge calculated from charge-

regulation model indicated that strong base treatment added more basic functional groups on carbon surface compared to weak base treatment.

The microbial growth experiment for *Pseudomonas putida* cells upon bacterial adhesion was conducted in conjunction with the analysis of surface physicochemical properties. The comparison associated with charge-regulation model among original solid and surface-modified solid (activated and silica sand) demonstrated an antimicrobial nature with either base or iron treatment on surfaces. This work supports our working hypothesis of charge-regulation about bioenergetics. The results indicated that the microbial activities may be controlled purposely to achieve desirable function via modifying the material surface properties.

1.4.3 Objective 3: Explore the Variation in Bioavailability of Ionizable Substrates Sorbed on Activated Carbon Due to the Charge-Regulated Effect

The effect of GAC surface properties on both adsorption capacity and microbial growth were evaluated via a combination of charge-regulation model and bioenergetics. Different ionizable substrates with acidic, basic and neutral functionality were used in the biological experiment to clarify the response of solid surface and cells upon adhesion.

In this study we provided an understanding of the bilateral effects of surface physicochemical properties on bacterial growth and bioavailability of sorbed ionizable substrates. The following sections described our findings about the influence of specific

charged surface on bacterial growth under different conditions in conjunction with (1) electrostatic analysis of surfaces, (2) biodegradation experiment. Chapter 2 proposed a quick and accurate approach to represent the physicochemcial properties of surfaces with functional groups using the measurable electrophoretic mobility. Such characterization on charged interfaces allows the development of charge-regulation model about the cellular bioenergetics with aerobic growth discussed in Chapter 3. Considering other potentially important aspects in biological process, especially under substrate limit condition, follows Chapter 4 revealed the influence of the charge-regulation effect on adsorption capability of activated carbon. Chapter 5 provided an overall viewpoint about the link we demonstrated that between the surface physicochemical nature of materials and the microbial bioenergetics activities.

References

Atrih A., Bacher G., Allmaier G., Williamson M. P. and Foster S. J. (1999) Analysis of peptidoglycan structure from vegetative cells of Bacillus subtilis 168 and role of PBP 5 in peptidoglycan maturation. J. Bacteriol. 181(13), 3956-3966.

Al-Degs S. Y., El-Barghouthi I. M.,El-Sheikh H. A., *et al*. (2008) Effect of solution pH, ionic strength, and temperature on adsorption behavior of reactive dyes on activated carbon. Dyes and Pigments. 77, 16-23.

Beveridge T. J. (1981) Ultrastructure, chemistry, and function of the bacterial wall. Int Rev Cytol. 72, 229-317.

Bowera C. K., McGuireb J., Daeschel M. A. (1996) The adhesion and detachment of bacteria and spores on food-contact surfaces. Trends in Food Sci. & Tech. 7 (5), 152-157.

Buonocore M, Wileman W, Brudevold F. (1956) A report on a resin composition capable of bonding to human dentin surfaces. J. Dent Res. 35, 846-851.

Carol K., Y. and John T. N. (1994) Anaerobic Biodegradation of Gasoline Oxygenates in Soils. Water Envir. Res. 66 (5), 744-752.

Czeslik, C., Winter, R. (2001) Effect of temperature on the conformation of lysozyme adsorbed to silica particles. Phys. Chem. Chem. Phys. 3, 235-239.

Gibbons R. J. (1984) Adherent interactions which may affect microbial ecology in the mouth. J. Dent. Res. 63, 378-385.

Gong, P., Szleifer, I. (2004) Competitive adsorption of model charged proteins: the effect of total charge and charge distribution. Journal of colloid and interface science, 278(1), 81-90.

Hong Y. and Brown D. G. (2006) Cell surface acid-base properties of Escherichia coli and Bacillus brevis and variation as a function of growth phase, nitrogen source and C:N ratio. Colloids Surf., B 50,112-119.

Hong, Y. and Brown, D. G. (2008) Electrostatic behavior of the charge-regulated bacterial cell surface. Langmuir 24, 5003-5009.

Hong, Y. and Brown, D. G. (2009) Variation in bacterial ATP level and proton motive force due to adhesion to solid surface. Applied and Envir. Microbiol. 75 (8), 2346-2353.

Hong Y. and Brown, D. G. (2010) Alteration of Bacterial Surface Electrostatic Potential and pH Upon Adhesion to a Solid Surface and Impacts to Cellular Bioenergetics. Biotechnol Bioeng. 105(5), 965-72.

Hong, Y. and Brown, D. G. (2011) Impact of the charge-regulated nature of the bacterial cell surface on the activity of adhered cells. J. of Adhesion Sci. and Tech. 25, 2199-2218.

Jones, C. W. (1988) Membrane-associated energy conservation in bacteria: a general introduction. In C. Anthony (ed.), Bacterial Energy Transduction. Academic press, New York.

Madigan M. T., Martinko J. M. and Parker, J. Brock Biology of Microorganisms. Prentice Hall, Upper Saddle River, NJ, (2000).

Mafu A. A., Plumety C., Deschênes, L., and Goulet J. (2011) Adhesion of pathogenic bacteria to food contact surfaces: Influence of pH of culture. International Journal of Microbiology, Article ID 972494, 10 pages.

Ninham B. W. and Parsegian V. A. (1971) Van der Waals forces in many-layered structures: Generalizations of the lifshitz result for two semi-infinite media. J. Theoret. Biol. 38 (1), 101-109.

Paula M. van Schie and Madilyn Fletcher. (1999) Adhesion of Biodegradative Anaerobic Bacteria to Solid Surfaces. Appl Environ Microbiol. 65(11), 5082-5088.

Petersen C. and Møller, L.B. (2000) Invariance of the nucleoside triphosphate pools of Escherichia coli with growth rate, J. Biol. Chem., 275, 3931-3935.

Ravichandran, S.; Talbot, (2000) Mobility of Adsorbed Proteins: A Brownian Dynamics Study. J. Biophys. J. 78(1), 110-120.

Terada A., Yuasa A., Kushimoto T., *et al*. (2006) Bacterial adhesion to and viability on positively charged polymer surfaces. Microbiology, 152, 3575-3583.

White, D. (2000) The physiology and biochemistry of prokaryotes. Oxford University Press, New York.

Zobell, C. E. (1943) The effect of solid surfaces upon bacterial activity. J. Bacteriol. 46, 39-56.

CHAPTER 2

CHARACTERIZATION OF CHARGE-REGULATED SURFACES USING ZETA POTENTIAL TITRATION DATA

CHAPTER 2 Characterization of Charge-Regulated Surfaces Using Zeta Potential Titration Data

2.1 Introduction

The surfaces of most materials in aqueous systems are charged due to the ionization of acidic (negatively-charged) and basic (positively-charged) functional groups. This ionization of functional groups results in surface charge variation as a function of the pH, and these surfaces are termed charge-regulated surfaces. There is a wide array of natural and manmade surfaces that exhibit charge-regulated properties, such as sand, glass, iron hydr(oxides), feldspar, aluminum hydroxide, clays, ion exchange resins, and bacteria. An interesting result with these surfaces is that when a charge-regulated surface approaches another surface, both the surface charge and surface electrostatic potential will vary as a function of separation distance (Ninham and Parsegian,1971; Brown and Hong, 2011;Hong and Brown, 2010; Chan *et al.*,1975; Healy *et al*., 1980); Hsu and Kuo, 1996; Prieve and Ruckenstein, 1977).

The charge-regulation effect is an important consideration in aqueous systems. When considering colloidal adhesion and interfacial forces, the surface charge and surface potential vary as a function of the ionization of the functional groups via the local pH immediately adjacent to the surface, which itself is a function of the surface electrostatic

potential and bulk pH through the Boltzmann distribution. Thus, the electrostatic forces will vary as a function of separation distance, with the effects related to the local ionization of the surface-bound functional groups. This results in a complex relationship for electrostatic interfacial forces due to the simultaneous variation in surface charge and potential. Many researchers neglect this effect (either actively or inadvertently) in DLVO modeling by using the simplification of a constant surface potential or surface charge.

Charge-regulated surfaces can also strongly influence the metabolic activity of attached bacteria. It has been shown that as a bacterium approaches a surface, the charge-regulation effect alters the local pH, which in turn affects cellular bioenergetics through changes in the energy stored in proton gradient across the cytoplasmic membrane (Brown and Hong, 2011; Hong and Brown, 2010, 2009). By manipulating the charge properties on the adhering surface using different acidic and basic functional groups, biological activity can be stimulated or inhibited (e.g., a passively-antimicrobial surface) Hong and Brown (2009; Albert, 2015).

Modeling of the charge-regulation processes requires quantification of the equilibrium constant and site density values for the surface functional groups. This data is typically obtained using acid/base (potentiometric) titration Hong and Brown (2006, 2008; Borrok 2004; Cox *et al*., 1999; Fein *et al*., 1997; Sokolov *et al.*, 2001). A drawback with this approach is that a high surface area is necessary to get a measurable pH response, and this thus requires a dense colloidal suspension of the material of interest, which may not

be possible with the material being examined. The suspension must also remain completely mixed and the use of a wide range of pH values can result in particle aggregation and settling. Finally, for porous and ion-penetrable materials (e.g., activated carbon and ion exchange resins) potentiometric titration will quantify groups throughout the material and cannot differentiate between those on the surface, which control the charge-regulation effect, and those in the interior, which do not.

Other methods have been developed for materials that don't lend themselves to potentiometric titration. For example, atomic force microscopy has been use to quantify surface charges of borosilicate glass and octadecyltrichlorosilane surfaces Jing and Bhushan (2013). And uranyl acetate and toluidine blue O dye, which interact with the functional groups, were used as probes to quantify the negatively-charged functional groups on membrane surfaces Tiraferri and Elimelech (2012). These methods, while able to quantify the number of functional groups, are not capable of providing the dissociation constants and thus are unsuited for use in characterizing surfaces for charge-regulation modeling.

Here we develop and demonstrate a simple method using zeta potential – pH titration data to obtain the equilibrium constants and site densities required to model charge-regulated surfaces. The benefit of this approach is that zeta potential measurements are readily obtained for colloidal particles (via electrophoretic mobility measurements) and granular material and planar materials (via streaming potential measurements). The goal

is to model the surface electrostatic potential and charge density as a function of pH. It should be noted that this does not require identification of all types of functional groups on the surface, but rather identification of a set of equilibrium constants and site densities that best represent the charge-regulated response of the surface. Here, develop the mathematical approach and demonstrate its ability to accurately represent charge-regulated surfaces using zeta potential-pH data for colloidal activated carbon.

2.2 Model Development

The goal of this work is to develop a mathematic approach for quantifying the functional group dissociation constants and site densities that best represent a given charge-regulated surface in an aqueous system. It is important to note that the goal is not to identify pK and N values for all functional groups on the cell surface, but rather to identify an appropriate set of values that allow representation of the charge properties of the cell surface across a specified pH range.

The charge-regulation model presented here follows the model proposed by Ninham and Parsegian Ninham and Parsegian (1971), with modifications to allow modeling of surfaces containing multiple functional groups (Hong and Brown 2010; Chan *et al*. 1975; Healy *et al*. 1980; Hsu and Kuo 1996; Prieve and Ruckenstein 1977; Hong and Brown 2008). Considering both acidic and basic sites on the surface, the surface charge is controlled by the following dissociation equilibria:

$$R_{ai}H \leftrightarrow R_{ai}^{-} + H^{+} \quad (1)$$

$$R_{bj}H^{+} \leftrightarrow R_{bj} + H^{+} \quad (2)$$

where R_{ai} are the acidic ionizable sites of type i, e.g., phosphoric, carboxylic, and hydroxyl groups, and R_{bj} is the basic ionizable sites of type j, e.g., amine group. The dissociation constants associated with these surface functional groups (K_{ai} and K_{bj}) are

$$K_{ai} = \frac{\left[R_{ai}^{-}\right]\left[H^{+}\right]_s}{\left[R_{ai}H\right]} \quad (3)$$

$$K_{bj} = \frac{\left[R_{bj}\right]\left[H^{+}\right]_s}{\left[R_{bj}H^{+}\right]} \quad (4)$$

where $\left[R_x\right]$ and $\left[R_xH\right]$ are the areal densities (molecules per unit surface area) of the dissociated and associated functional groups and $[H^+]_s$ is the molar concentration of hydrogen ions near the surface. $[H^+]_s$ is calculated using the Boltzmann distribution,

$$[H^{+}]_s = [H^{+}]\exp\left(-\frac{e\psi_s}{kT}\right) \quad (5)$$

where $[H^+]$ is the molar concentration of hydrogen ions in the bulk solution; ψ_s is the surface electrostatic potential (V); e is the electron charge (1.602×10^{-19} C); k is the Boltzmann constant (1.381×10^{-23} J/K); and T is the temperature (K).

Given these dissociation equations, N_{ai} and N_{bj} are then defined as the number of acid sites of type j and base sites of type j per unit surface area:

$$N_{ai} = \left[R_{ai}^{-}\right] + \left[R_{ai}H\right] \tag{6}$$

$$N_{bj} = \left[R_{bj}\right] + \left[R_{bj}H^{+}\right] \tag{7}$$

The surface charge density (σ, C per unit surface area) is then equal to the total number of positively charged sites minus the total number of negatively charged sites:

$$\frac{\sigma}{e} = \sum_{j}\left[R_{bj}H^{+}\right] - \sum_{i}\left[R_{ai}^{-}\right] \tag{8}$$

Equations (3) to (8) can be combined to yield an expression for the surface charge density as a function of the dissociation of the surface acid/base functional groups:

$$\frac{\sigma}{e} = \sum_{j}\left[\frac{[H^{+}]N_{bj}}{[H^{+}] + K_{bj}\exp\left(\frac{e\psi_s}{kT}\right)}\right] - \sum_{i}\left[\frac{K_{ai}N_{ai}}{K_{ai} + [H^{+}]\exp\left(\frac{-e\psi_s}{kT}\right)}\right] \tag{9}$$

The surface charge density can also be calculated via the Grahame equation Israelachvili (1992):

$$\sigma = \pm\sqrt{2\varepsilon_o\varepsilon kT\sum_{m} n_{rm}\left\{\exp\left(-\frac{z_m e\psi_s}{kT}\right) - 1\right\}} \tag{10}$$

which relates the charge and potential of an isolated surface in a given electrolyte composition. The choice of sign in equation 10 is dictated by the sign of ψ_s, i.e., if $\psi_s < 0$ then $\sigma < 0$, and visa versa.

For the approach used here, the zeta potential (ζ) of the surface is experimentally determined as a function of solution pH. Then using ζ as a surrogate for ψ_s, equations 9 and 10 are used to calculate the pK and N values. Considering the p^{th} data point in the ζ-pH titration curve, the difference between the surface charges ($\Delta\sigma$) calculated via the Grahame equation (equation 10) and via the Charge-Regulation equation (equation 9) is

$$\Delta\sigma_p = \sum_j \left[\frac{[H^+]_p N_{bj}}{[H^+]_p + K_{bj} \exp\left(\frac{e\zeta_p}{kT}\right)} \right] - \sum_i \left[\frac{K_{ai} N_{ai}}{K_{ai} + [H^+]_p \exp\left(\frac{-e\zeta_p}{kT}\right)} \right] \mp \sqrt{2\varepsilon_o \varepsilon kT \sum_m n_{rmp} \left\{ \exp\left(-\frac{z_m e\zeta_p}{kT}\right) - 1 \right\}} \tag{11}$$

The goal is to minimize the sum-of-squares residual (R) across all the titration data points by optimizing the values of K_{bj}, N_{bj}, K_{ai}, and N_{ai}, where

$$R = \sum_p \left(\Delta\sigma_p\right)^2 \tag{12}$$

This was accomplished by coding equation 12 in C++ and linking it to the non-linear parameter estimate code PEST (Watermark Numerical Computing). Given the

experimental titration data and the values of i and j (i.e., the number acid and basic functional groups used to represent the surface) PEST provides the best-fit values of K_{bj}, N_{bj}, K_{ai}, and N_{ai}, along with their covariance matrix and 95% confidence intervals. The optimal values of i and j are selected to minimize R, and this will be discussed further in the results section.. Once the K and N values are known, equations 9 and 10 are then used to determine the surface potential as a function of pH.

2.3. Materials and Methods

Granular activated carbon (GAC) (*Evoqua Water Technologies,* LLC) was used as the surface in this study. The GAC particles were dried at 60 ℃ overnight prior to use. GAC fines were obtained by crushing the dry granular particles in a mortar, suspending the crushed particles in 50 mL of electrolyte solution and allowing the coarser particles to settle out of solution. The supernatant was used directly for zeta potential analysis with a Zetasizer Nano ZS (Malvern Instruments). Size analysis showed that the resulting fines had a mean effective diameter of 0.37 microns.

The electrolyte was 10 and 100 mM NaCl, with the solution purged continuously with N_2 gas. The pH was adjusted with N_2-purged 0.1 M NaOH and 0.1 M HCl. The zeta potential was calculated from electrophoretic mobility data using the Smoluchowski equation (McLaughlin *et al.,* 1981). The data obtained at each titration point include: pH, ζ, and bulk concentrations of Na^+ and Cl^-.

2.4 Results and Discussion

The zeta potential results for the 10 mM NaCl and 100 mM NaCl experiments are shown in Figures 2.1(A) and 2.2(A) and the corresponding surface charge densities, calculated from the Grahame equation, are shown in Figures 2.1(B) and 2.2(B). It was not known *a priori* how many acidic and basic groups are required to best-represent the surface. To determine this, the charge-regulation model was fit to the data using different numbers of acidic (i.e., K_a) and basic (i.e., K_b) groups and the best-fit model results are presented as the lines in Figures 2.1 and 2.2. The residuals (equation 12) for these different model fits are provided in Figures 2.1(C) and 2.2(C) and they demonstrate that the model is best-fit with a three functional groups. While additional groups could be fit to the data, no further refinement in the model fit was observed.

The best-fit K and N values for the model run with one acidic and two basic groups (i.e., 1 K_a and 2 K_b) are presented in Table 2.1. The parameter K_{a1} represents a negatively-charged functional group and K_{b1} and K_{b2} represent positively-charged functional groups. The surface charge is based on the difference in charge between these groups (i.e., $\sigma = \sigma_{b1} + \sigma_{b2} - \sigma_{a1}$) and it's the difference, not the absolute value of the charges that is important. Thus, the solutions provided by this approach are not necessarily unique and uniqueness is not required to represent the charge-regulated properties of the surface. This can be seen in the correlation coefficient matrix for the 100 mM data presented in Table 2.2,

where there is strong correlation between the parameters, especially the N_{a1} and N_{b2} parameters.

The charge-regulation model is not a function of the solution ionic strength, and the parameters determined from zeta potential data at one ionic strength should, theoretically, be able to represent the surface at other ionic strengths. This was examined by simulating the 10 mM NaCl data using the K and N values obtained from the 100 mM NaCl data, and vice versa. The results are shown in Figure 2.3 as the dashed lines, and they provide a fairly good representation of the zeta potential as a function of pH.

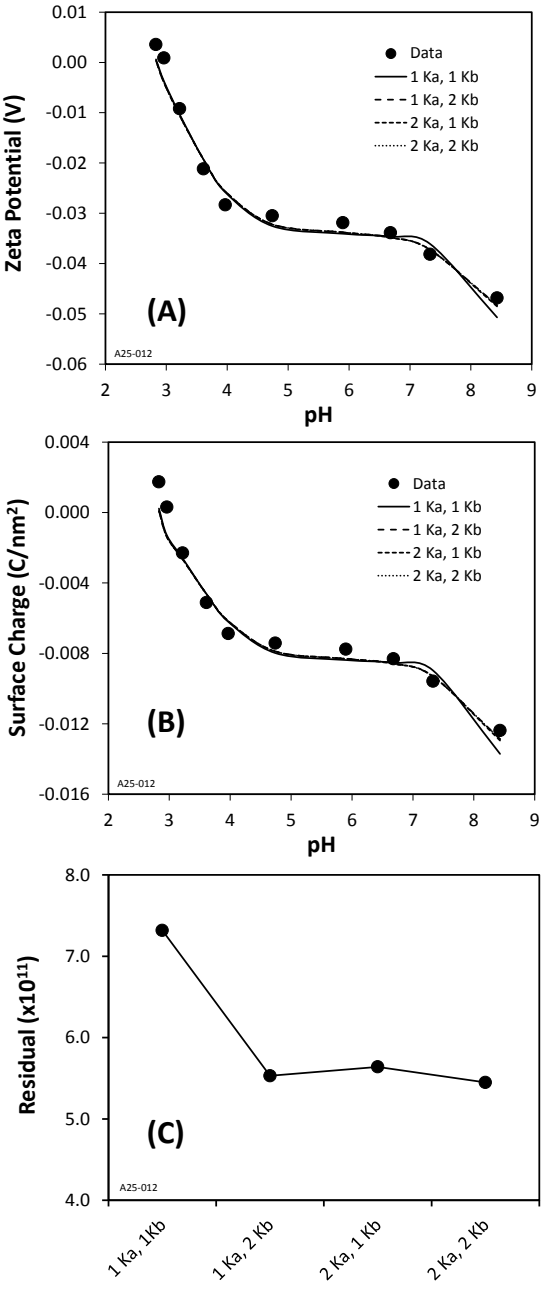

Figure 2.1 - Data and model results for activated carbon suspended in 10 mM NaCl. (A) Zeta potential data (symbols) and model results (lines) for different combinations of functional groups. (B) Surface charge density calculated using the Grahame equation (symbols) and charge-regulation model (lines). (C) Residual for model fits.

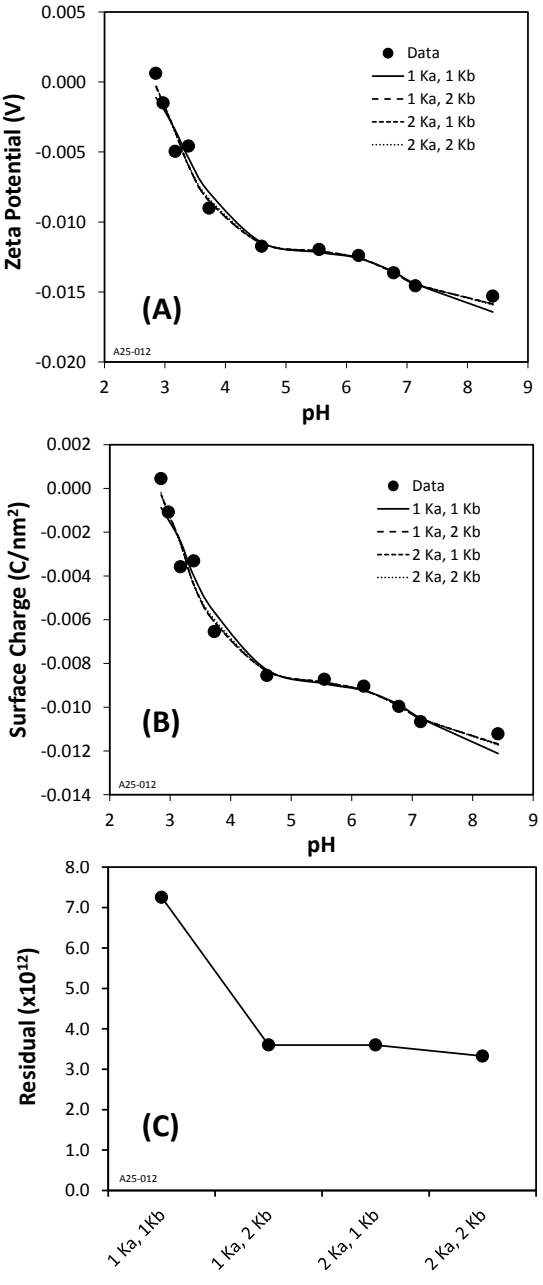

Figure 2.2 - Data and model results for activated carbon suspended in 100 mM NaCl. (A) Zeta potential data (symbols) and model results (lines) for different combinations of functional groups. (B) Surface charge density calculated using the Grahame equation (symbols) and charge-regulation model (lines). (C) Residual for model fits.

Table 2.1 - Example pK and N values for the 1 Ka, 2 Kb model fits. K values are presented as pK = -log (K).

	10 mM	**100 mM**	**Combined 10 mM & 100 mM**
pK_{a1}	0.647	2.84	0.837
N_{a1} (#/nm^2)	9.20	0.108	6.08
pK_{b1}	7.49	6.77	6.95
N_{b1} (#/nm^2)	0.0474	0.0187	0.0272
pK_{b2}	11.5	11.6	12.1
N_{b2} (#/nm^2)	9.10	0.0348	6.00

Table 2.2 - Correlation coefficient matrix for the 1 K_a, 2 K_b model fit to the 100 mM data.

	K_{a1}	**N_{a1}**	**K_{b1}**	**N_{b1}**	**K_{b2}**	**N_{b2}**
K_{a1}	1.000	-0.982	0.305	0.239	0.241	-0.866
N_{a1}	-0.982	1.000	-0.230	-0.179	-0.181	0.843
K_{b1}	0.305	-0.230	1.000	0.973	0.932	-0.707
N_{b1}	0.239	-0.179	0.973	1.000	0.968	-0.679
K_{b2}	0.241	-0.181	0.932	0.968	1.000	-0.664
N_{b2}	-0.866	0.843	-0.707	-0.679	-0.664	1.000

Table 2.3 - Correlation coefficient matrix for the 1 K_a, 2 K_b model fit to the combined 10/100 mM data.

	K_{a1}	**N_{a1}**	**K_{b1}**	**N_{b1}**	**K_{b2}**	**N_{b2}**
K_{a1}	1.000	0.169	0.229	0.149	0.153	-0.169
N_{a1}	0.169	1.000	0.981	0.999	0.959	-1.000
K_{b1}	0.229	0.981	1.000	0.978	0.931	-0.982
N_{b1}	0.149	0.999	0.978	1.000	0.959	-0.999
K_{b2}	0.153	0.959	0.931	0.959	1.000	-0.959
N_{b2}	-0.169	-1.000	-0.982	-0.999	-0.959	1.000

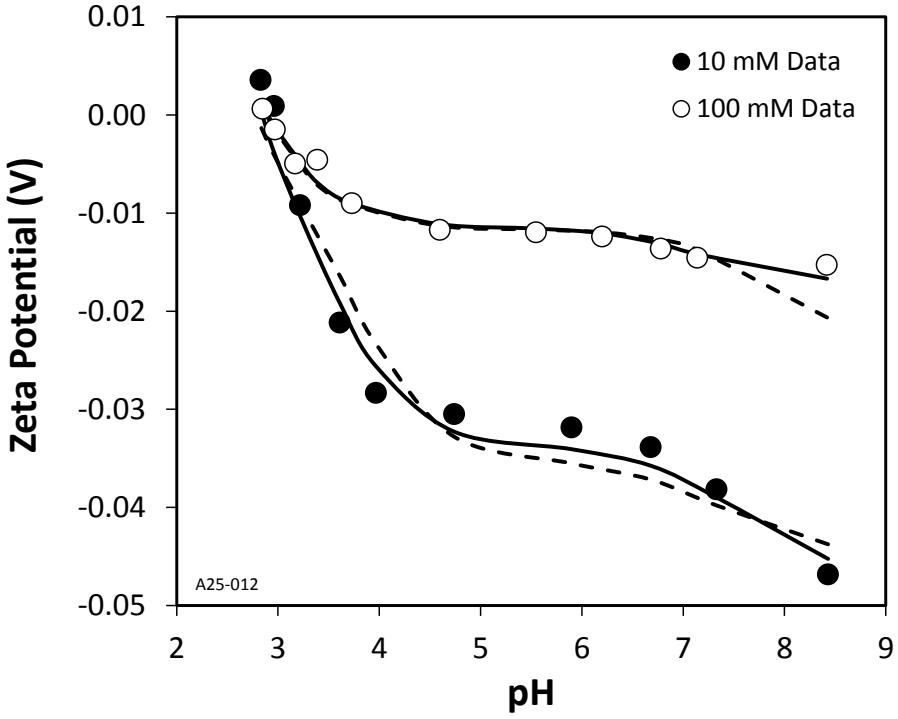

Figure 2.3 - Symbols are experimental data at two NaCl concentrations. Dashed lines represent the model fits using the K and N parameters from the opposite data sets (e.g., K and N values obtained from 10 mM data are then used to model the 100 mM data). Solid lines are the best-fit model results when simultaneously fitting both data sets. Associated K and N values are provided in Table 2.1.

Further refinement in the charge-regulation parameters can be obtained by fitting both data sets simultaneously to a single set of K and N values. This provides a more robust estimate of the K and N values for a given surface and would tend to remove the effects of experimental noise in a single data set. Model parameters were determined for the combined 10 mM and 100 mM NaCl data sets and the results are presented in Figure 2.4.

As expected, the surface charge density, which is not a function of the electrolyte concentration, aligns for both data sets (circles in Figure 2.4(B)). Multiple combinations of acidic and basic functional groups were fit to the data, and examination of the residuals provided in Figure 2.4(C) indicates that the system is best represented with three functional groups. This is similar to the results in Figures 2.1 and 2.2, with the refinement that the three groups are composed of one acidic and two basic functional groups. The best-fit K and N values are presented in Table 2.1. As with the model results with the single data sets, the parameters are not unique, and there is high correlation between the parameters, as shown in the correlation coefficient matrix in Table 2.3. The zeta potential curves, modeled using the parameters in Table 2.1, are plotted in Figure 2.3, and it is seen that the simultaneously-fit K and N values provide a more robust fit to the data across the different ionic strengths than those when using K and N values determined from one ionic strength. These results demonstrate that the K and N values determined at one ionic strength can provide an adequate representation of the zeta potential at other ionic strengths. Determination of the K and N values using

data at multiple ionic strengths, however, provides a more robust representation of the charge-regulated surface.

To demonstrate the applicability of this approach to other materials, we applied it to aluminum oxide, iron oxide, Feldspar and silica sand. The zeta potential titration curves for these materials, shown in Figure 2.4, are in agreement with published data Stumm and Morgan (1996) and show a range of responses, from acidic (sand and Feldspar) to basic (iron oxide and aluminum oxide) functionalities. The charge-regulation model results are shown in Figure 2.4 and Table 2.4, and in all cases the model was able to adequately represent the zeta potential response as a function of pH.

Overall, the modeling approach described herein provides a rapid means to obtain parameters for modeling the charge-regulated response of a solid surface. While the parameters are not necessarily unique, uniqueness itself is not a requirement for modeling a charge-regulated surface. If identification of functional groups is necessary, this approach could be combined with potentiometric titration to further refine the results Hong and Brown (2006 and 2008). Additionally, the approach described herein could be further refined to allow determination of ion sorption to surfaces through inclusion of ion-exchange stoichiometry Hong and Brown (2008).

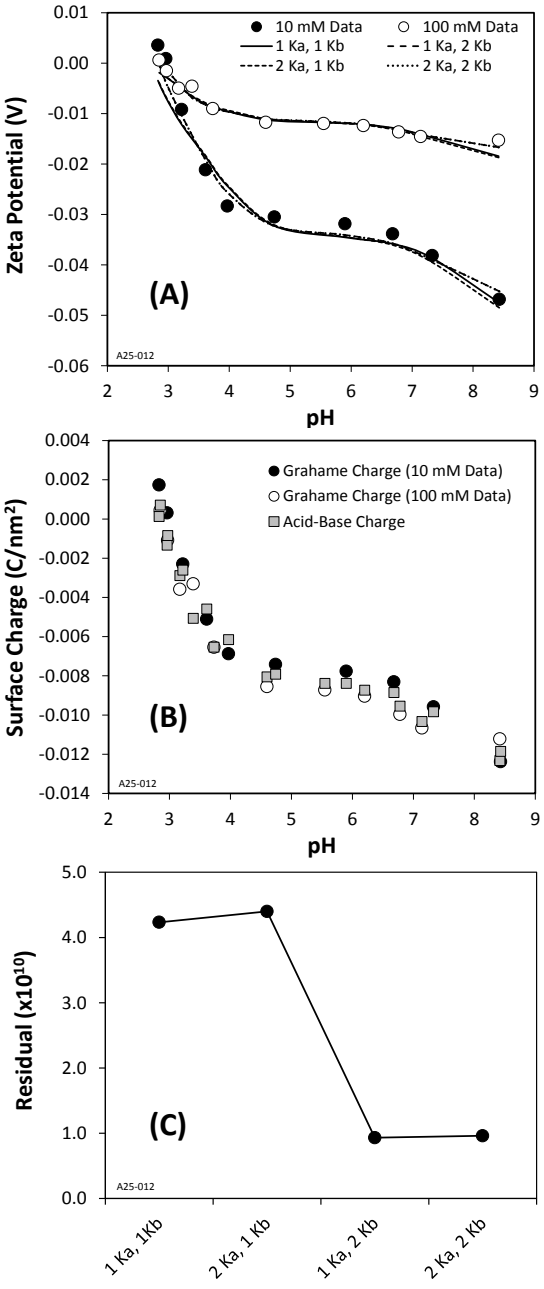

Figure 2.4 - Data and model results for activated carbon suspended in both 10 mM and 100 mM NaCl. (A) Zeta potential data (symbols) and model results (lines) for different combinations of functional groups. (B) Surface charge density calculated using the Grahame equation (symbols) and charge-regulation model with one acidic and two basic functional groups (lines). (C) Residual for model fits.

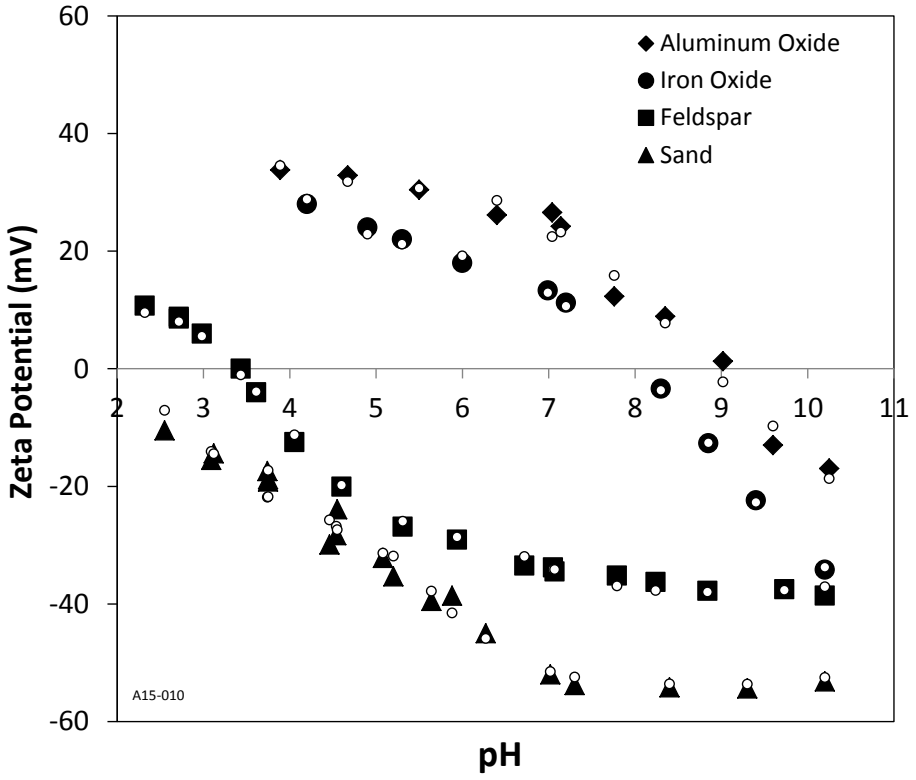

Figure 2.5 - Zeta potential and model results for aluminum oxide, iron oxide, Feldspar and silica sand. Data obtained at a NaCl concentration of 100 mM and titrations carried out similar to that with the activated carbon. Solid symbols are zeta potential and hollow symbols are the charge-regulation model fits. Associated K and N values are presented in Table 2.4.

Table 2.4 - pK and N data for minerals presented in Figure 2.4.

Sand	pK_{a1}	2.75
	N_{a1} (#/nm^2)	0.0383
	pK_{a2}	5.16
	N_{a2}(#/nm^2)	0.0532
Feldspar	pK_{a1}	3.72
	N_{a1} (#/nm^2)	0.0643
	pK_{b1}	6.42
	N_{b1} (#/nm^2)	0.0202
Iron Oxide	pK_{a1}	4.42
	N_{a1} (#/nm^2)	0.0393
	pK_{a2}	7.52
	N_{a2}(#/nm^2)	0.0303
	pK_{b1}	9.04
	N_{b1} (#/nm^2)	0.0687
Aluminum Oxide	pK_{a1}	4.30
	N_{a1} (#/nm^2)	0.0170
	pK_{a2}	7.74
	N_{a2}(#/nm^2)	0.0338
	pK_{b1}	9.41
	N_{b1} (#/nm^2)	0.0641

References

Ninham, B.W. and Parsegian, V.A. (1971) Electrostatic potential between surfaces bearing ioniable groups in ionic equilibrium with physiologic saline solution. Journal of Theoretical Biology 31, 405-428.

Brown, D.G. and Hong, Y. (2011) Impact of the Charge-Regulated Nature of the Bacterial Cell Surface on the Activity of Adhered Cells. Journal of Adhesion Science and Technology 25(17), 2199-2218.

Hong, Y. and Brown, D.G. (2010) Alteration of bacterial surface electrostatic potential and pH upon adhesion to a solid surface and impacts to cellular bioenergetics. Biotechnology and Bioengineering 105(5), 965-972.

Chan, D., Perram, J.W., White, L.R. and Healy, T.W. (1975) Regulation of surface potential at amphoteric surfaces during particle-particle interaction. Journal of the Chemical Society, Faraday Transactions I 71, 1046-1057.

Healy, T.W., Chan, D. and White, L.R. (1980) Colloidal behaviour of materials with ionizable group surfaces. Pure and Applied Chemistry 52, 1207-1219.

Hsu, J.-P. and Kuo, Y.-C. (1996) The electrostatic interaction force between a charge-regulated particle and a rigid surface. Journal of Colloid and Interface Science 183, 194-198.

Prieve, D.C. and Ruckenstein, E. (1977) Role of surface chemistry in particle deposition. Journal of Colloid and Interface Science 60(2), 337-348.

Hong, Y. and Brown, D.G. (2009) Variation in bacterial ATP level and proton motive force due to adhesion to a solid surface. Applied and Environmental Microbiology 75(8), 2346-2353.

Albert, L.S. (2015) Effects of surface properties on the charge-regulated bioenergetic response of attached bacteria: Exploration within the framework of the chemiosmotic theory. Ph.D. Dissertation, Lehigh Universithy, Bethlehem, PA.

Hong, Y. and Brown, D.G. (2006) Cell surface acid-base properties of *Escherichia coli* and *Bacillus brevis* and variation as a function of growth phase, nitrogen source and C:N ratio. Colloids and Surfaces B: Biointerfaces 50(2), 112-119.

Hong, Y. and Brown, D.G. (2008) Electrostatic behavior of the charge-regulated bacterial cell surface. Langmuir 24(9), 5003-5009.

Borrok, D. (2004) Proton and Cd adsorption onto natural bacterial consortia: Testing universal adsorption behavior1. Geochimica et Cosmochimica Acta 68(15), 3231-3238.

Cox, J.S., Smith, D.S., Warren, L.A. and Ferris, F.G. (1999) Characterizing heterogeneous bacterial surface functional groups using discrete affinity spectra for proton binding. Environmental Science & Technology 33, 4515-4521.

Fein, J.B., Daughney, C.J., Yee, N. and Davis, T.A. (1997) A chemical equilibrium model for metal adsorption onto bacterial surfaces. Geochimica et Cosmochimica Acta 6(16), 3319-3328.

Sokolov, I., Smith, D.S., Henderson, G.S., Gorby, Y.A. and Ferris, F.G. (2001) Cell surface electrochemical heterogeneity of the Fe(III)-reducing bacteria *Shweanella putrefaciens*. Environmental Science & Technology 35(2), 341-347.

Jing, D. and Bhushan, B. (2013) Quantification of surface charge density and its effect on boundary slip. Langmuir 29(23), 6953-6963.

Tiraferri, A. and Elimelech, M. (2012) Direct quantification of negatively charged functional groups on membrane surfaces. Journal of Membrane Science 389, 499-508.

Israelachvili, J. (1992) Intermolecular and Surface Forces, Academic Press, San Diego.

Stumm, W. and Morgan, J.J. (1996) Aquatic Chemistry, John Wiley & Sons, Inc., New York.

CHAPTER 3

IMPACT OF THE CHARGE-REGULATION EFFECT ON MICROBIAL GROWTH OF ATTACHED BACTERIA

CHAPTER 3 Impact of the Charge-Regulation Effect on Microbial Growth of Attached Bacteria

3.1 Introduction

Bioremediation has been considered as a wide application of microbial processes or microorganisms in degrading contaminants and cleaning-up ground water, lagoons, industrial wastewater. It offers a variety of advantages over typical chemical or physical processes in such aspects as cost-effective treatment or environmentally benign manufacturing, especially emphasizing the destruction of pollution rather than the disposal (Baker and Herson, 1994). Biodegradation process could remove the pollutants permanently, and is potentially coupled with physical or chemical process. An increasing amount of studies on biological treatment on organic carbon have been performed successfully considering both microbial growth and contaminant removal efficiency (Boopathy, 2000).

The operating state of microbiological processes is governed by metabolic activity levels. This study is to explore a way to link the charge-regulation nature of solid surfaces to cellular bioenergetics of attached bacteria as shown in Figure 3.1 (Brown and Hong, 2011; Hong and Brown, 2010; Hong and Brown, 2009; Hong and Brown, 2008; Hong and Brown, 2006). Our working hypothesis proposes that the proton distribution at the both surfaces of cells and attached solid surfaces could be altered upon adhesion due to

charge-regulation effect, and that would change the metabolic activity by shifting the local pH on charge-regulated surfaces. Previous studies in our lab showed that the cellular ATP levels of adhered cells under non-growth conditions were either enhanced or decreased by adhering to materials containing acid/base functional groups at the surface. Further, this variation in metabolic activities of cells was demonstrated through our charge-regulation model to be associated with the dissociation groups and site density of those surface functional groups. While the effect of physiochemical properties of adhered surfaces on microorganism growth and biodegradation efficiency remains unclear.

In this study, we examined the aerobic microbial activity levels of *Pseudomonas putida* in growth in the presence of activated carbon and energy source, which was combined with the characterization of surface positive/negative charge and the evaluation of surface modification. Our charge-regulation model was developed, where the microbial growth and relative bioremediation application involving bacterial adhesion was related to surface electrostatic nature. Through charge-regulation model, surface electrostatic properties were represented in terms of dissociation species and site density of functional groups on surfaces. The variation in the attached growth rates of *P. putida* with original solid and surface-modified solid indicated an obvious antimicrobial nature associated with materials with specific surface treatment. The results demonstrated that the bioactivities can be potentially controlled to optimize material manufacture and to achieve desirable functions in environmental clean-up remedies.

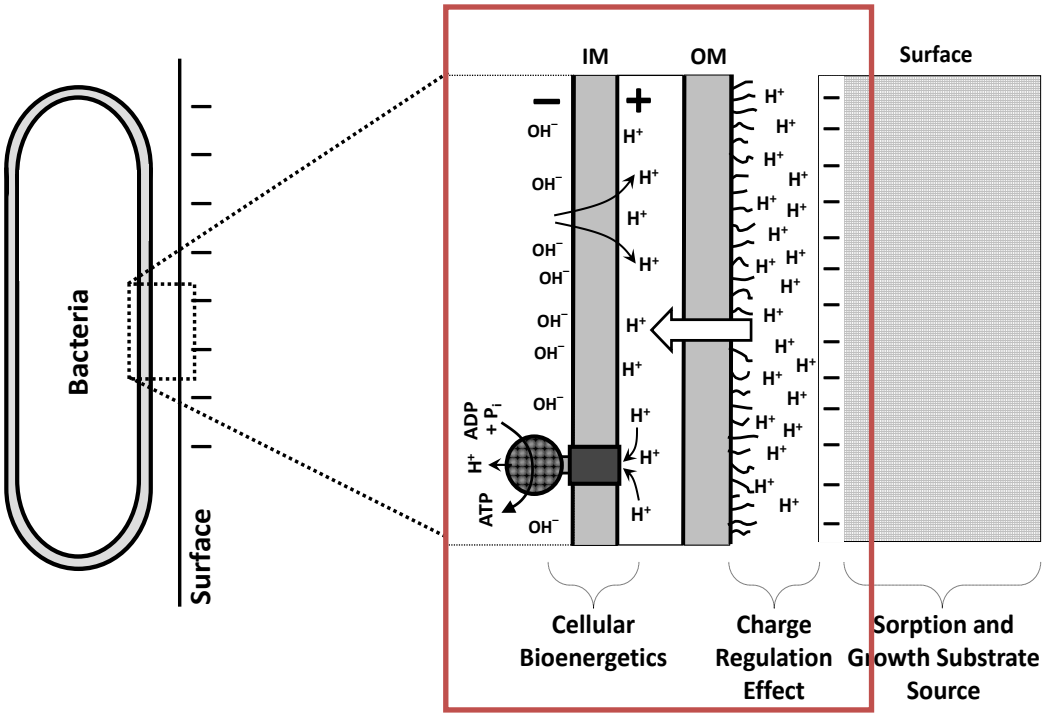

Figure 3.1 - The figure described the combined processes of the Gram-negative bacteria cell approaching a negatively-charged solid surface. The box indicates how the charge-regulation effect is governed and related to metabolic activities, on which this chapter focuses. The charge-regulation model in conjunction with cellular bioenergetics is capable of simulating the response of attached microorganisms when attached to surfaces of specific physicochemical properties. Protons are pumped across the inner membrane (IM) with respiration process, building up proton gradient across the cell membrane resulting in the proton motive force (Δp). Local ion distribution on outer membrane (OM) may vary due to electron neutrality once approaching to a positively or negatively charged surface. Basically, we hypothesize that charge-regulated surface induces an alteration in proton gradient across cell membrane upon adhesion, and accordingly affects both local pH and metabolic activity levels as well as microbial growth.

3.2 Materials and Approaches

3.2.1 Microorganism Culture

The gram-negative bacteria strain *P. putida* (ATCC 31947) obtained from the American Type Culture Collection, was used in this study. The bacteria were grown at 30℃ in 250 mL of of Luria Bertini broth (LB broth, Fisher Scientific). Cells were harvested in the exponential phase, then mixed with 15% glycerol, and stored at -86℃ using the glass bead method (Jones J., Pell P.A. *et al*., 1991; Hong Y. and Brown D.G., 2008; Hong Y. and Brown D.G., 2009).

An aerobic culture at exponential growth phase was prepared by inoculating the *P. putida* cells from the frozen stock in a minimal growth media at 30℃ for 36 hours. The sterilized media composition includes 5.44 g/L KH_2PO_4, 0.5 g/L NH_4Cl, and 0.6 mL/L mineral salt stock solution (containing 10 g/L $MgSO_4 \cdot 7H_2O$, 0.1 g $CaCl_2 \cdot 2H_2O$, 0.4 g $FeSO_4 \cdot 7H_2O$, 1.0 g $MnCl_2 \cdot 2H_2O$ in 1 L deionized water). The pH was adjusted to 7.2 with 3 N NaOH. The bacterial working culture was grown to the late exponential phase and ready for either inoculation in respirometer bioreactors or washing procedure for cell surface characterization.

The bacteria washing /starvation process was applied to achieve a clean surface on cells prior to zeta potential measurement on cell surface. The working culture was then harvested and washed twice by centrifuging the suspension at 3500×g for 15 minutes

each at room temperature, followed by re-suspending the bacterial cells in phosphate buffer solution (PBS, 0.258g KH_2PO_4 and 0.470g K_2HPO_4 in 1 L deionized water with the pH adjusted to 7.2 using 3 N NaOH). The bacteria suspension was placed on a rotary shaker for a 24-hour starvation period that washed, and re-suspended in specific electrolyte solution for the sequential electrophoretic mobility test. This starvation process was to deplete the microbial energy reserves. The cell suspensions were diluted with the test solution to a concentration of approximately 10^6 cells/mL determined by Acridine Orange direct counts (Hobbie J.E., Daley R.J., *et al.*, 1977).

3.2.2 Solid Surface Preparation and Treatment

Materials selected as solid surfaces included standard mineral sand (Ottawa sand ASTM 50-70, d_{10} = 0.5 mm, d_{50} = 0.72 mm), surface-modified sands and activated carbons (from Evoqua Water Technologies, LLC). The standard sand was first soaked in 1.0 M HCl solution for 12 hours to remove the mineral impurities and then under running tap water for 4 hours. The sand was then washed in 18.2 MΩ deionized (DI) water for at least three times and then dried at 60 ℃.

The clean and dry sand of 200 g was treated with 100 mL of 0.2 M ferric chloride ($FeCl_3 \cdot 6H_2O$). Ferric hydroxide (goethite) was then precipitated in the solution by increasing the pH to 7.5 using 6 M NaOH. The sand was kept mixing in a shaker at 60 ℃ for 6 hours after which it was dried in the oven for 24 hours at 105 ℃. The coated sand

batches were finally washed using DI water flow, dried again in the oven at 105℃ for 48 hours and ready for the application as solid surfaces.

All three granular activated carbons (GACs) were obtained from Evoqua Water Technologies, LLC. Untreated coconut-based GAC carries neutral surface. Weak base and strong base treatment processes were applied on the untreated GAC to produce positively charged surface. The strong base- and weak base-treated GACs were expected to bear more positive charged functional groups at the surface, which could be validated later by our surface charge calibration. All activated carbons were grinded to US mesh 200x325, followed by wet sieving, drying 60℃ overnight and ready to use in both electrophoresis mobility measurement and respirometer experiment.

3.2.3 Surface Characterization

The solid surfaces were observed using the Scanning Electron Microscope (SEM) / Energy Dispersive X-ray Spectroscopy (EDS). Surface elemental mapping was performed using Energy Dispersive X-ray Analysis to confirm the iron coating on the sand surface and nitrogen element distribution on the carbon surface.

The electrophoretic mobility/zeta potential of surfaces (includes both the bacterial cell and solid surfaces) along with titration across a wide pH range (2.5-9.5) was obtained from a Nano Zetasizer ZS (Malvern Instruments, Worcestershire, UK). Solid fines were obtained either by crushing dried solids or from the washing procedure. Bacterial cells

(prepared as mentioned earlier) were reuspended in 50 mL of 10 mM NaCl solution after cell washing.

The best-fit charge-regulation model was used to determine the values of dissociation constant (pK) and charge density (N) of each functional group at the surface (approach described in Chapter 2). The model we were using was based on the Poisson-Boltzmann equation, which describes the electrostatic potential in the bulk as a function of distance away from another surface. By combining with the numerical optimization code PEST (Watermark Numerical Computing), the surface pK and N values were accessible.

3.2.4 Respirometer System

The real-time oxygen uptake of the bacterial cells was determined from the Pulse-Flow respirometer system (PF-8000), which consists of biological reaction vessels, a control module that contains the pneumatic and electronic controls for oxygen or gas flow, and a computer. The inlet oxygen pressure flowing into the control module when is constant operating in the aerobic mode in which oxygen uptake is measured. We designed and fabricated the bioreactors that were sealed and kept in water bath at 20℃. The respirometer system was operated in aerobic mode keeping 8 mL 1 N sodium hydroxide in each reactor to absorb the carbon dioxide given off during respiration.

10 ml of the working microorganism culture (as description in microorganism cultivation) was inoculated to 690 mL minimal growth media at 20℃. Either benzoic

acid or lactose was used as the sole carbon and energy source in microbial growth experiment. Benzoic acid has a acidic functionality; while lactose exhibits neutral functionality. No obvious adsorption on sands was detected in preliminary tests. The adsorption isotherm of activated carbon is determined prior to the respirometer experiment to keep the same aqueous concentration in all reactors per test.

3.3 Results and Discussions

3.3.1 Surface Characterization of Activated Carbon

The Scanning electron microscope (SEM) analysis of the untreated activated carbon and surface-modified carbon particles (weak base- and strong base-treated carbons) showed the structure of activated carbon particles. Both weak and strong base treatment was to add more basic functional groups, which contained more nitrogen element. Energy Dispersive X-ray Spectroscopy (EDS) analysis here was carried out and determined the element distributions of carbon, oxygen and nitrogen at the surfaces of weak base- and strong base-treated activated carbons (Figure 3.3 and 3.4). Untreated GAC had no detectable nitrogen on its surface (Figure 3.2). The strong base-treated carbon surface carried nitrogen at a weight ratio of 3.65%, which was higher than that of weak base treated carbon surface at 1.78%. Oxygen content remained constant on surfaces of untreated and base-treated activated carbon at a weight percentage of 10.0 approximately, which is consistent as previous reports (Mangun *et al*., 1999; Shafeeyan *et al*., 2010).

The surface charge on activated carbon surfaces was calculated from zeta potential profile as a function of pH through the charge-regulation model (as described in Chapter 2) , which was obtained from electrophoretic mobility experiment. The result demonstrated that the strong base treated activated carbon carried more basic functional groups at the surface, which results in a shift in the isoelectric point (IEP) of the carbon surfaces from approximately 2.5 for both untreated carbon and weak base treated carbon surfaces to around 4.2 for the strong base treated carbon surface (Figure 3.5). The calculated values of surface charge may be underestimated due to more fresh surfaces exposed to bulk solution result from crushing procedure.

3.3.2 Surface Characterization of Sands

The SEM/EDS analysis of the iron coated sand showed the surface structure of iron coated sand particles (Figure 3.6). The distributions of major elements at the surfaces were determined by EDS as listed in Table 3.1. The iron weight ratios of regular sand and iron coated sand are 0.86% and 34.84%, respectively. Meanwhile, environmental electron microscope (ESEM) micrographs provided a visual comparison of surface iron coating between both original silica sand and iron-coated sand particles (Figure 3.7), which indicated a roughly 15% coverage of iron at the surface.

This iron treatment resulted in a shift in the isoelectic point (IEP) of the sand from 1.5 for the regular sand to approximately 8 (Figure 3.8). Thus, regular sand particles exhibited a

net negatively charge surface, while the surface-modified (iron coated) sand showed more positive properties.

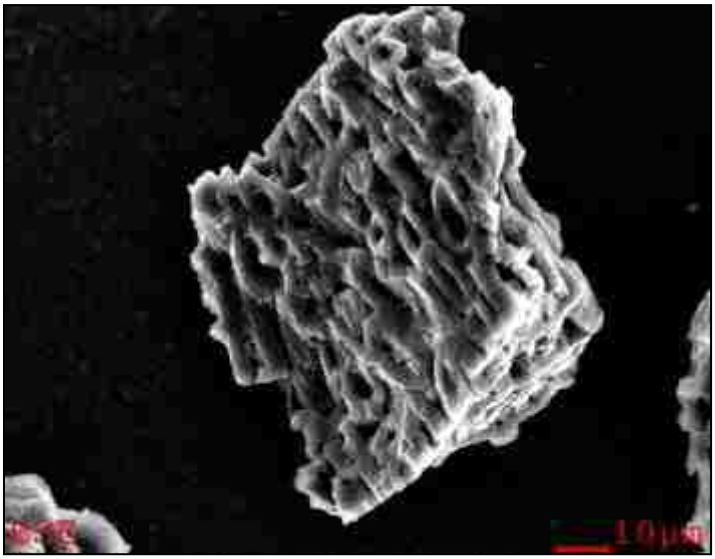

Element	Wt %	At %
Carbon (C)	90.76	92.90
Oxygen (O)	09.24	07.10
Nitrogen (N)	0.00	0.00

Figure 3.2 - Scanning electron microscope (SEM) / Energy Dispersive X-ray Spectroscopy (EDS) images of untreated activated carbon particles. EDS analysis determined the element distributions of carbon (C) and oxygen (O), respectively. No nitrogen (N) was detected on untreated carbon surface.

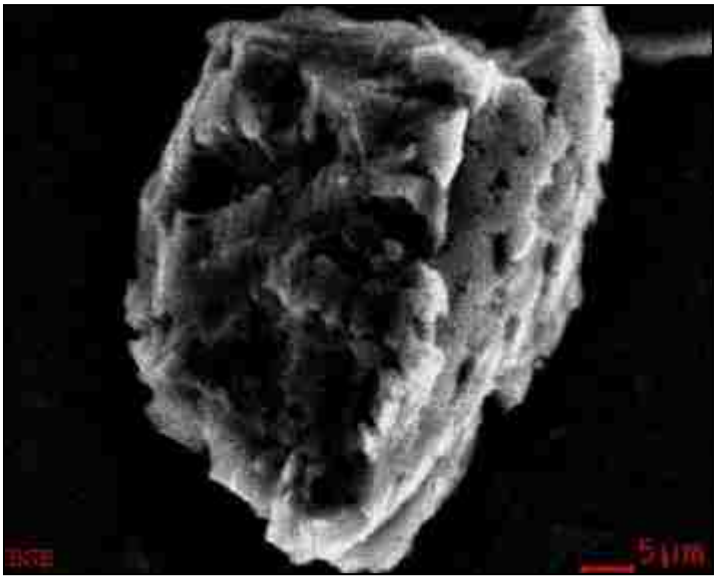

Element	Wt %	At %
Carbon (C)	88.12	90.63
Oxygen (O)	10.10	07.80
Nitrogen (N)	01.78	01.57

Figure 3.3 - SEM/EDS images of weak base treated activated carbon particles. EDS analysis determined the element distributions of carbon (C), oxygen (O) and nitrogen (N), respectively. The weight percentage of nitrogen detected at the carbon surface was 1.78%.

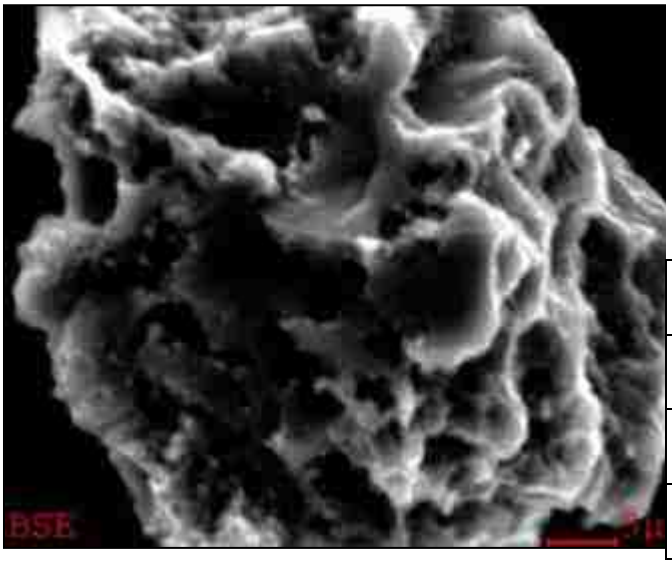

Element	Wt %	At %
Carbon (C)	85.64	88.46
Oxygen (O)	10.72	08.31
Nitrogen (N)	03.65	03.23

Figure 3.4 - SEM/EDS images of strong base treated activated carbon particles. EDS analysis determined the element distributions of carbon (C), oxygen (O) and nitrogen (N), respectively. The weight percentage of nitrogen detected at the carbon surface was 3.65%.

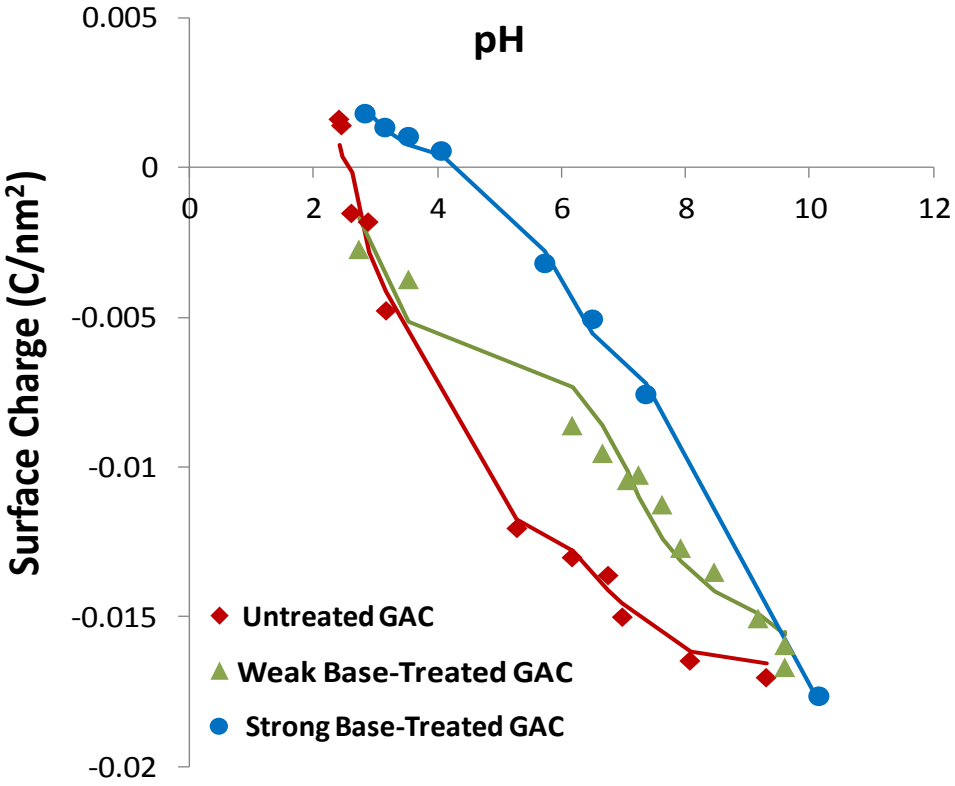

Figure 3.5 - Surface characterization of three granular activated carbons (GACs) including untreated GAC, and both weak base- and strong base-treated GACs.

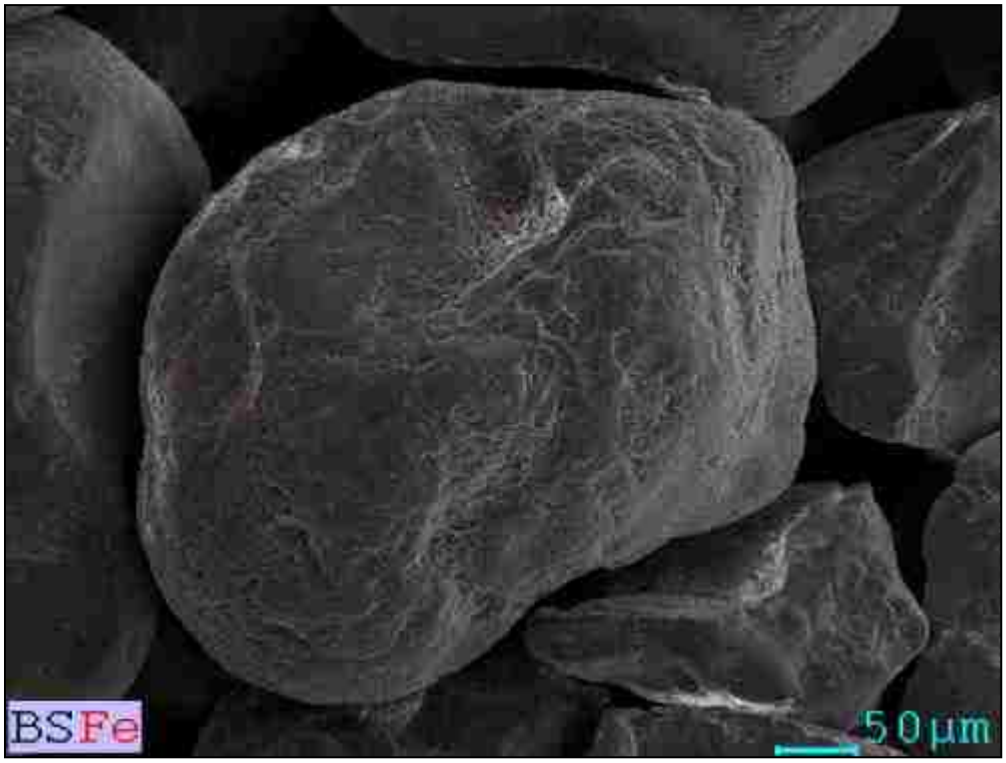

Figure 3.6 - Scanning electron microscope (SEM) / Energy Dispersive X-ray Spectroscopy (EDS) images showing iron-coated sand particles. SEM allowed mapping the iron distribution on sand particles and the EDS element analysis with demonstrating the element distribution as in Table 3.1.

Table 3.1 - Energy Dispersive X-ray Spectroscopy (EDS) element analysis comparing the iron coated sand to the regular sand. The significant increase in iron weight ratio validated the iron element coating on sand surface.

	Regular Silica Sand		**Iron Coated Sand**	
Element	**Wt %**	**At %**	**Wt %**	**At %**
O	34.95	48.72	31.56	52.01
Na	00.59	00.57	00.52	00.60
Mg	00.64	00.59	00.84	00.91
Al	01.99	01.64	01.80	01.76
Si	56.99	45.26	26.81	25.18
P	03.99	02.87	03.64	03.10
Fe	**00.86**	**00.34**	**34.84**	**16.45**

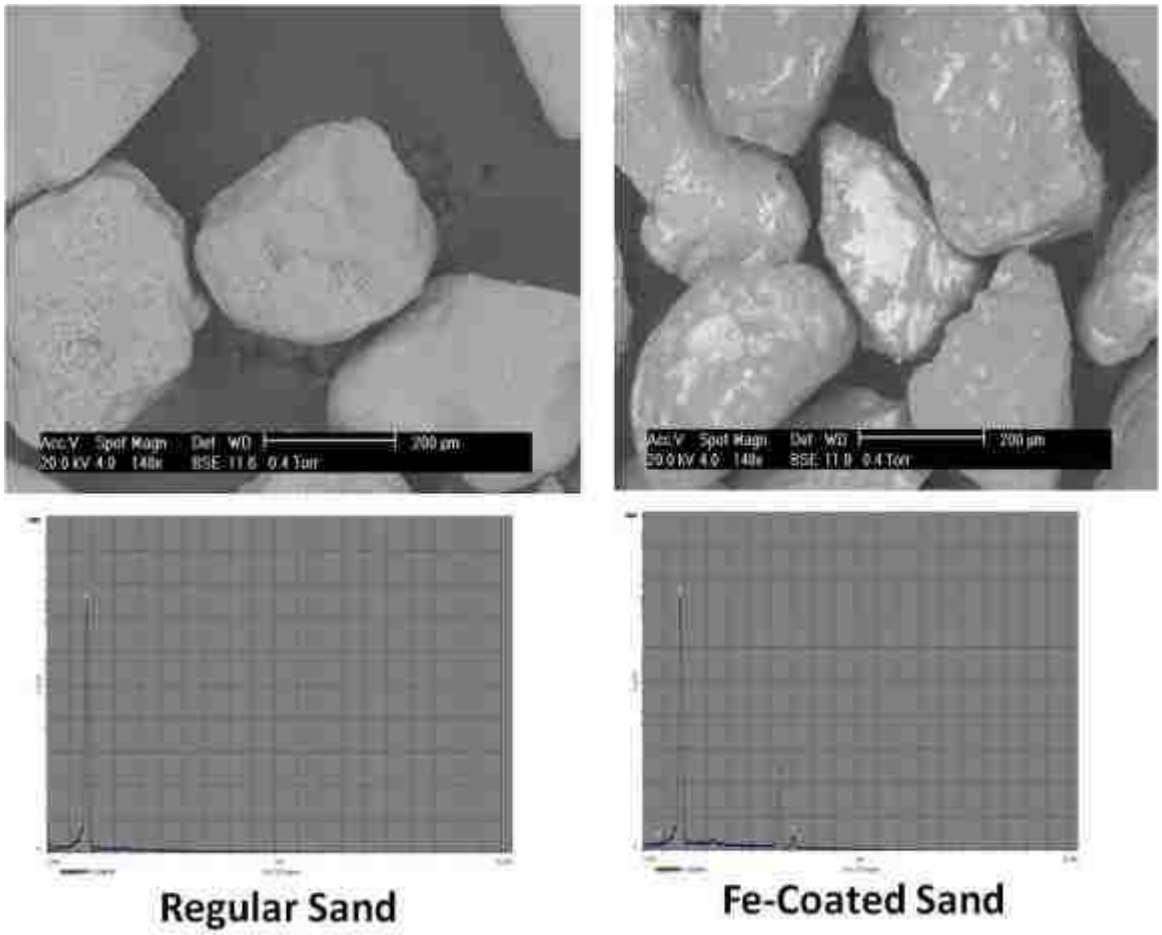

Figure 3.7 - Environmental electron microscope (ESEM) micrographs showing both original silica sand and iron-coated sand particles imaged at 20 kV. Particles size ranges from 260 to 350 μm. Scale bar length 200 μm.

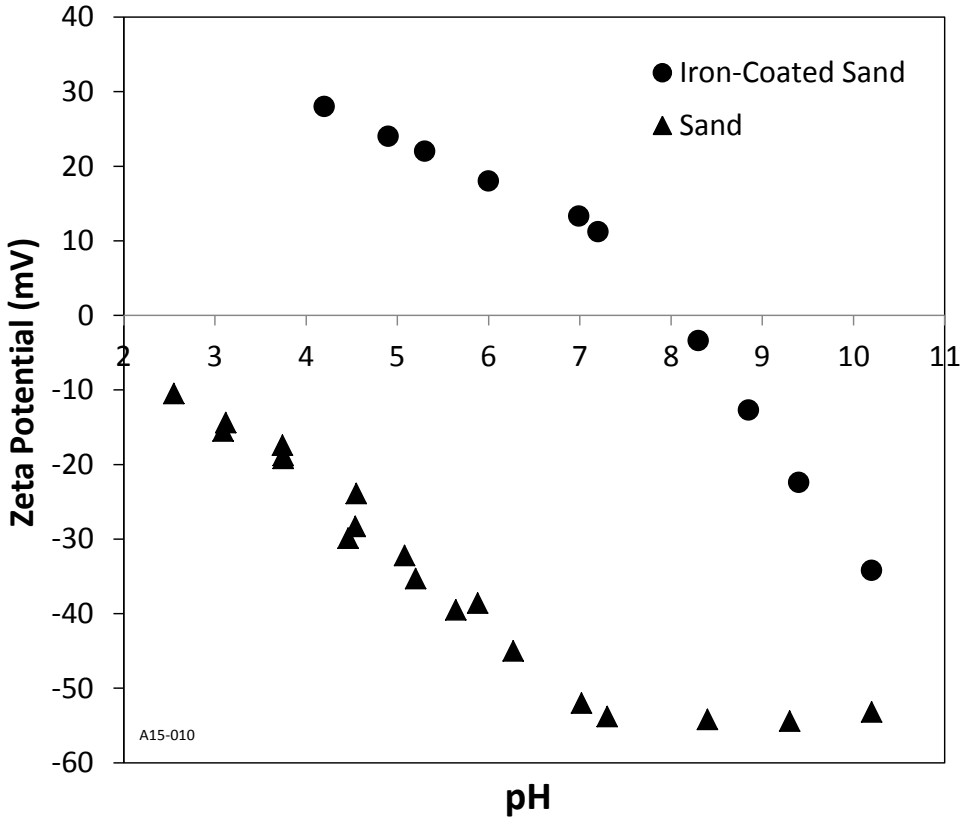

Figure 3.8 - Zeta potential of the regular and iron-coated sand suspended in 10 mM NaCl electrolytes. A large shift in the isoelectric point (IEP) was detected between regular sand and iron coated sand.

3.3.3 Surface Characterization of *Pseudomonuas putida* Cells

The zeta potential profile along with pH for *P. putida* cells are shown in Figure 3.9. The Cell suspension was determined to have an isoelectric point (IEP) near 2.3. It was constant with the values in previous literature (Rijnaarts *et al*., 1994), which reported IEP 2~3. The bacterial cell surface could be considered as negative charged surface. This acidic surface pH was due to the negatively-charged surface of cellular lipid molecule layers and the local proton distribution adjacent to cell surface.

3.3.4 Determination of the Values of K and N for Surfaces

The surface zeta potential profile from electrophretic mobility experiment was used to calculate the K and N values for each specific functional group at the surface from Grahame equation. To best represent the pH-dependent charge properties of the surfaces, the charge-regulation model was fit to the data using different numbers of acidic/basic functional groups. The parameter K_{ai} represents a negatively-charged functional group, and K_{bi} represent positively-charged functional groups. The best-fit K and N values for the model run with multiple charged surfaces are presented in Table 3.2.

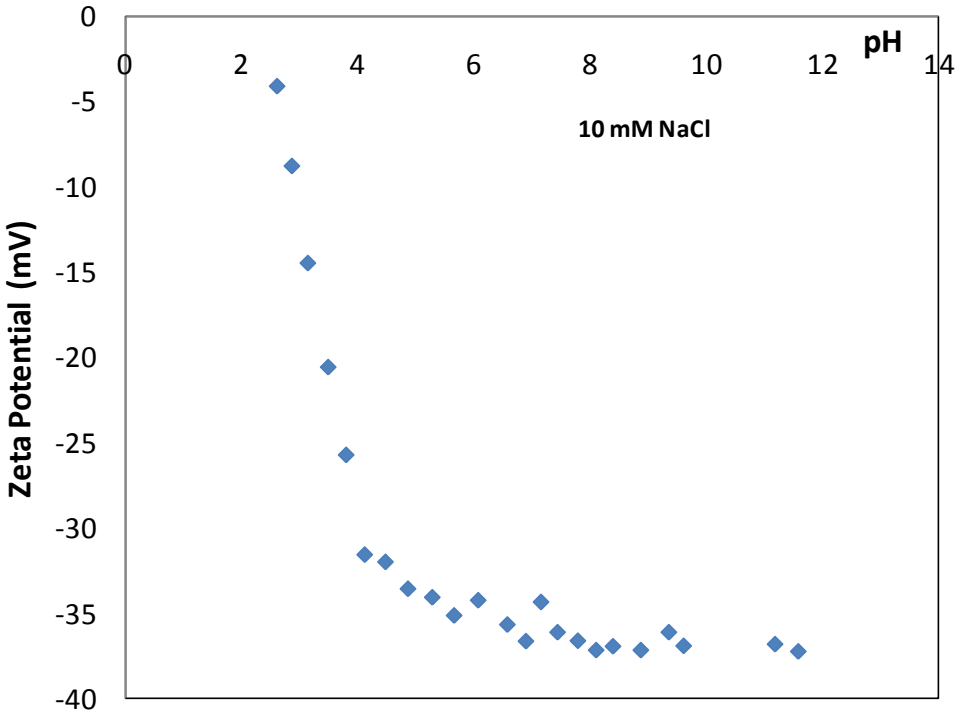

Figure 3.9 - Zeta potential of the *P. putida* cell suspension in 10 mM NaCl. The isoelectric point (IEP) was determined to be around 2.3, which is following the reports in previous literature (Rijnaarts *et al*., 1994) indicating a pH range of 2~3.

Table 3.2 - Best-fit pK and N values for acidic (i.e., K_a) and basic (i.e., K_b) sites for selected surfaces presented in Figure 3.5, 3.8 and 3.9. Parentheses indicate 95% confidence intervals. Resulting model fits using these values are presented in Figure 3.10. K values are presented as pK = -log(K).

Sand	**pK_{a1}**	2.75
	N_{a1} (#/nm^2)	0.0383
	pK_{a2}	5.16
	N_{a2}(#/nm^2)	0.0532
Iron Oxide	**pK_{a1}**	4.42
	N_{a1} (#/nm^2)	0.0393
	pK_{a2}	7.52
	N_{a2}(#/nm^2)	0.0303
	pK_{b1}	9.04
	N_{b1} (#/nm^2)	0.0687
P. putida	**pK_{a1}**	3.09
	N_{a1} (#/nm^2)	0.048
	pK_{b1}	9.01
	N_{b1} (#/nm^2)	0.0059
Untreated Activated Carbon	**pK_{a1}**	0.647
	N_{a1} (#/nm^2)	9.20
	pK_{b1}	7.49
	N_{b1} (#/nm^2)	0.0474
	pK_{b2}	11.5
	N_{b2} (#/nm^2)	9.10

3.3.5 Electrostatic Behavior between Cells and Solid Surfaces upon Bacterial Adhesion

The pK and N values of activated carbons and *P. putida* cell surfaces were used to estimate bacterial response upon adhesion to untreated and surface-modified carbon surfaces. Both theory development and simulation approach were described in Chapter 2. Figure 3.10(a) demonstrated the cell surface pH shifting associated with separation distance from solid surfaces. The results showed that at neutral bulk pH at 7, the *P. putida* cell surface pH values vary from 5.9 to 6.2 when approaching untreated carbon and base-treated carbons.

When cells approach and attach onto activated carbon surfaces, the local pH shifted and separated depending on the solid surface physicochemical properties. Due to the nature of electroneutrality, the strong base treated carbon with more positively charged functional groups at the surface resulted in charge-regulated surfaces with higher surface pH than that of either weak base treated carbon or untreated carbon. Specially, the strong base treated carbon induced a higher local in the vicinity of the cell and solid surfaces, and showed basic properties during bacterial adhesion. Considering our hypothesis about charge-regulation effect on bioenergetics, the higher local pH would directly decline metabolic activity levels and inhibit bacterial growth. Such antimicrobial nature of base treated activated carbon was further verified in the following biodegradation experiment.

Figure 3.10(b) showed the pH profile of charge-regulated surface for *P. putida* cells as a strong function of basic charge density at the surface of strong base-treated activated carbon as well as the separation distance. Known the functional group dissociation, the simulation also taken into account of the site number at carbon surfaces throughout the charge-regulation model, which allowed the estimation on how surface pH varied responding to charge density at the solid surface. The results showed a higher cell surface pH always associated with the surfaces carrying more basic functional groups / positive charge.

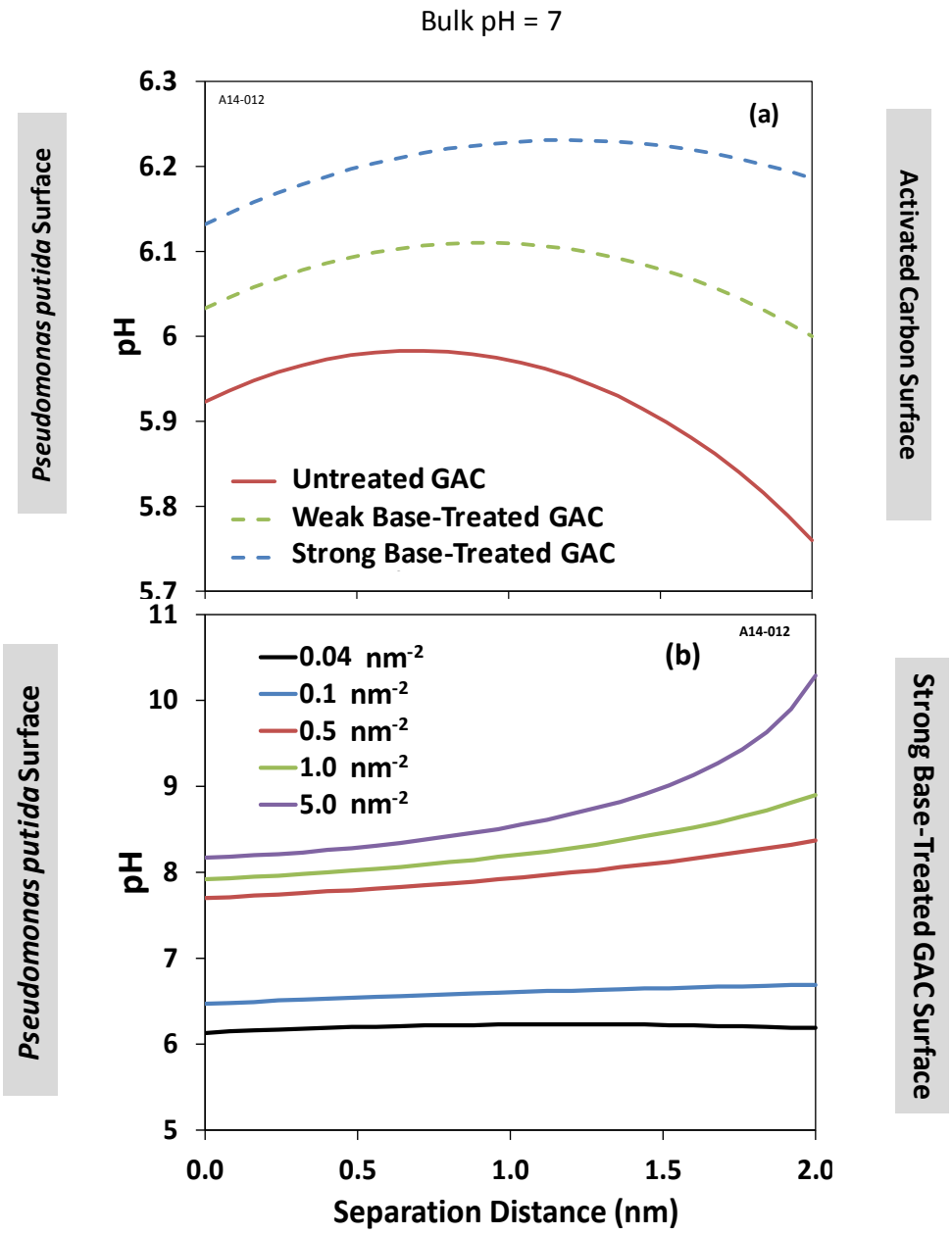

Figure 3. 10 - The electrostatic behavior of *P. putida* upon approaching charged surfaces of three activated carbons. (a) Charge-regulated surface pH shifting between cell and carbon surfaces as a function of separation distance. (b) The variation in pH profile as a strong function of basic site density at the strong base-treated activated carbon.

3.3.6 Biological Stoichiometry for Benzoate and Lactose

To experimental represent the charge-regulation and to link the oxygen utilization to bacterial growth, the biological stoichiometry for benzoic acid and lactose was calculated. Bacterial growth involves two basic reactions, one for energy production and the other for cellular synthesis. When cells use a substrate (electron-donor) for synthesis, a portion of its electrons (f_e) is transferred to oxygen (electro-acceptor) to produce energy to send the other portion of electron (f_s) into bacterial cells. f_e and f_s support the framework for partitioning the electron donor between cell synthesis and energy production. Thus, it could be calculated as

$$f_e + f_s = 1 \tag{1}$$

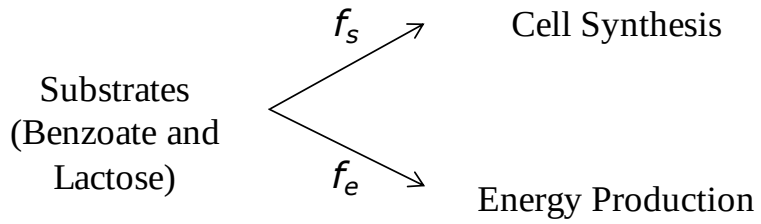

The overall equation for net synthesis of bacteria using either benzoate as electron donor and nitrate as electron acceptor is calculated from Equation (1) as follows:

$$R = f_e R_a + f_s R_c - R_d \tag{2}$$

Where, R is the overall reaction, R_a is the acceptor half-reaction, R_c is the cell half-reaction, and R_d is the donor half-reaction.

The overall reaction for benzoate can be determined by the followings. R_d for benzoate:

$$\frac{1}{5}CO_2 + \frac{1}{30}HCO_3^- + H^+ + e^- \rightarrow \frac{1}{30}C_6H_5COO^- + \frac{13}{30}H_2O \quad (3)$$

R_a for oxygen:

$$\frac{1}{4}O_2 + H^+ + e^- = \frac{1}{2}H_2O \quad (4)$$

R_c for *P. putida* cells:

$$\frac{1}{5}CO_2 + \frac{1}{20}HCO_3^- + \frac{1}{20}NH_4^+ + H^+ + e^- = \frac{1}{20}C_5H_7O_2N + \frac{9}{20}H_2O \quad (5)$$

By substituting Equation 3, 4 and 5 in Equation 2, we could develop the overall equation as:

$$0.0333C_6H_5COO^- + 0.25f_eO_2 + (0.05 - 0.05f_e)NH_4^+ \rightarrow (0.05 - 0.05f_e)C_5H_7O_2N + 0.2f_eCO_2 + (0.05f_e + 0.0167)H_2O + (0.05f_e - 0.0167)HCO_3^- \quad (6)$$

Given the Gibb's free energy for organic ($\Delta G^{0'}$) and electron accepter (R_a) are 27.34 and -78.72 kJ/e^-eq, respectively, we can determine the values of f_e (0.41) and f_s (0.59) for planktonic cells. By putting f_e and f_s into Equation 6, the overall reaction (planktonic cells) is developed as:

$$0.0333C_6H_5COO^- + 0.1025O_2 + 0.0295NH_4^+ \rightarrow 0.0295C_5H_7O_2N + 0.082CO_2 + 0.0038HCO_3^- + 0.0372H_2O \quad (7)$$

Based on Equation 7, the oxygen yield (ratio of oxygen utilization in grams to the mass of the substrate in grams) is calculated as in Equation 8.

$$Y_{O_2} = (g\ \ oxygen / g\ \ benzoate) = \frac{0.25 \times 32}{0.0333 \times 144} f_e$$

$$= 1.668 f_e = 1.668 - 1.668 f_s \tag{8}$$

Similarly, the overall reaction that includes energy generation and synthesis with lactose was developed in the same pattern.

$$\begin{aligned} &0.02083 C_{12}H_{22}O_{11} + 0.25 f_e O_2 + (0.05 - 0.05 f_e) HCO_3^- + (0.05 - 0.05 f_e) NH_4^+ \\ &\rightarrow (0.05 - 0.05 f_e) C_5 H_7 O_2 N + (0.05 + 0.2 f_e) CO_2 + (0.05 f_e + 0.1792) H_2 O \end{aligned} \tag{9}$$

$$Y_{O_2} = (g\ \ oxygen / g\ \ lactose) = \frac{0.25 \times 32}{0.02083 \times 342} f_e$$

$$= 1.123 f_e = 1.123 - 1.123 f_s \tag{10}$$

For both substrates, the oxygen utilization as a function of f_e are presented in Figure 3.11. The results demonstrated that the oxygen utilization rate can be affected by both bacterial growth rate (via cellular metabolic activity level, which governs how fast the substrate can be consumed) and energy production coefficient f_e (the linear relationship shown in Figure 3.11). The increase in total oxygen utilization of bacteria potentially resulted from

the lower energy production coefficient (f_e), which occurs when adhering onto surfaces containing basic functional groups (e.g. base-treated GAC and iron-coated sand).

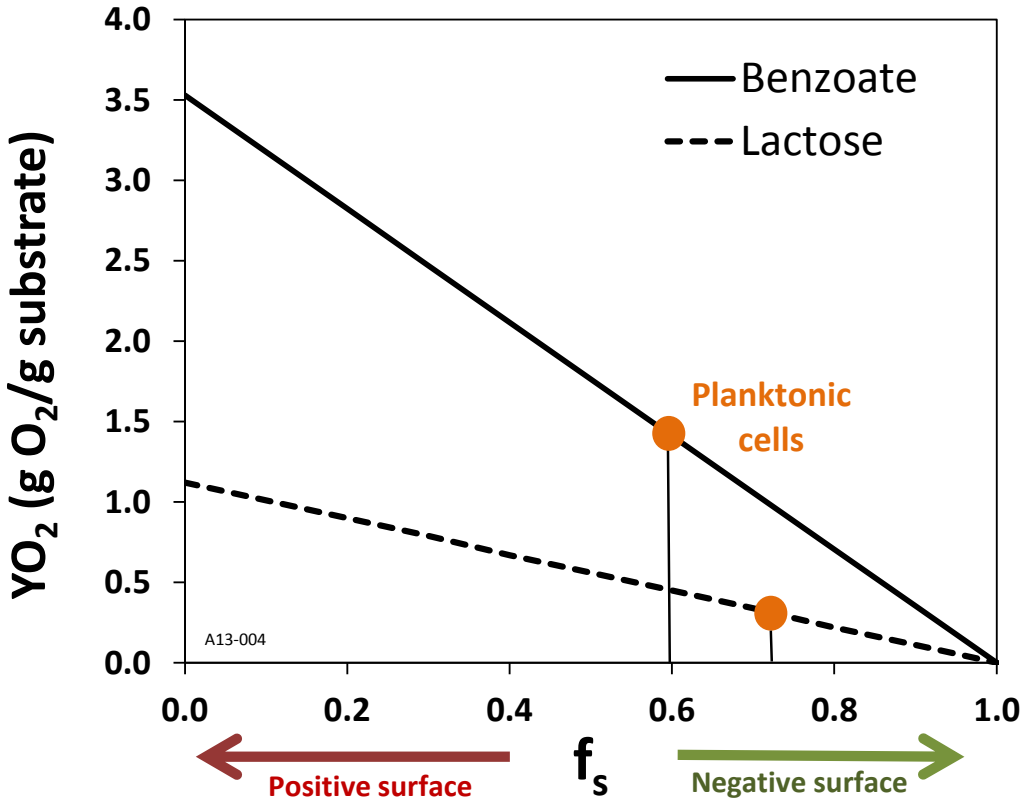

Figure 3.11 - The oxygen utilization as a function as energy production coefficient (f_e), which indicating the metabolic activity level of adhered bacteria. The results are based on theoretical calculation, showing that the values of f_e for planktonic cells with benzoate and lactose are 0.59 and 0.72, respectively. It also indicates that the microbial oxygen utilization increases with declined f_e when cells approach positive surfaces (e.g. base-treated GAC and iron-coated sand); while, the oxygen uptake volume would drop with a higher bacterial activity level and f_e value when adhering to negatively charged surface (e.g. untreated GAC and regular sand).

3.3.7 Respirometer Result for Activated Carbons

Our working hypothesis predicts that a variation in surface pH due to charge-regulation effect will have a corresponding impact on metabolic activity level upon bacterial adhesion. The decreased surface pH will ultimately result in enhanced bacterial growth while the increased surface pH will induce inhibited bacterial growth.

In this study, the bacterial growth rate is represented in terms of real-time oxygen uptake volume, which was obtained from respirometer system. The oxygen uptake volume as a function of pH with the initial concentrations of 250 and 20 mg/L was determined as in Figure 3.12. The *P. putida* cells were cultured in the sole carbon source (benzoic acid) minimal media as described in the method section. The results indicated a varied biodegradation rate of the bacteria grown with untreated or surface modified/base-treated activated carbons. The bacterial growth rate with untreated carbon was significantly higher than that with the two base-treated carbon surfaces at both concentrations of benzoic acid, which is in agreement with our hypothesis.

In the presence of 250 mg/L of benzoic acid, the bacterial cells with the weak base- and strong base-treated carbons were growing at similar growth rate slop within the first 30 hours after adding the substrate. Thereafter both base-treated carbons exhibited obvious antimicrobial effect and the growth rate was slowed down. After 50-hour growth duration, the bacteria with three carbons all grew fast due to the multiple layers of biofilm formation, which isolated microorganisms from affected by surface properties. For

benzoic acid at 20 mg/L, the results indicated a similar trend that the strong base treatment on carbon surface restrained metabolic activities once bacterial adhesion occurred with mixing together carbon surfaces, bacterial cells and growth media. The results clearly demonstrated that the positively charged surfaces resulting from base surface treatment directly inhibited cellular bioenergetics.

3.3.8 Respirometer Result for Sands

The regular sand and iron-coated sand were prepared and also used in conducting respirometer experiment. The sorption isotherm of substrates could be a potential factor affecting bacterial growth rate due to the high sorption capability of activated carbon (will discuss in Chapter 4). To make our study straightforward on the charge-regulation effect about bacterial growth, sands were selected to be the solid surfaces due to its minor sorption capability and universality.

Six reactors (100 mL) containing high concentrations of substrate (either 2 mg/L or 4 mg/L) were used in this study. Instead of ionizable weak acid substrate (benzoic acid), here lactose was chosen as the sole carbon source, which exhibits neutral functionality. Sufficient lactose of either 50 or 100 mg per reactor was added to each 25 mL minimal media in each sealed bioreactor, together with fixed amount (60 g) of either regular sand or iron-coated sand. Compared to the results with regular sand, the biodegradation rate of bacteria cells attached to iron-coated sand was significantly declined during the first 200-hour period with 50 mg lactose and the first 300-hour period with 100 mg lactose,

respectively (Figure 3.13). Thereafter, the oxygen uptake levels associated with both regular sand and iron-coated sand turned out to the similar level due to the huge amount of planktonic cell growth and biofilm formation.

Moreover, the total oxygen utilization volumes of cells with charged surfaces turned out to be close after the growth duration of 60 ~ 100 hours for activated carbon and of 200 ~ 300 hours for sands due to the huge amount of planktonic cell growth and biofilm formation. The increase in total oxygen utilization of bacteria for surface-modified materials potentially resulted from the lower energy production coefficient (f_e), which inhibited the metabolic activities of bacteria when adhered onto strong base-treated GAC as described in Figure 3.11.

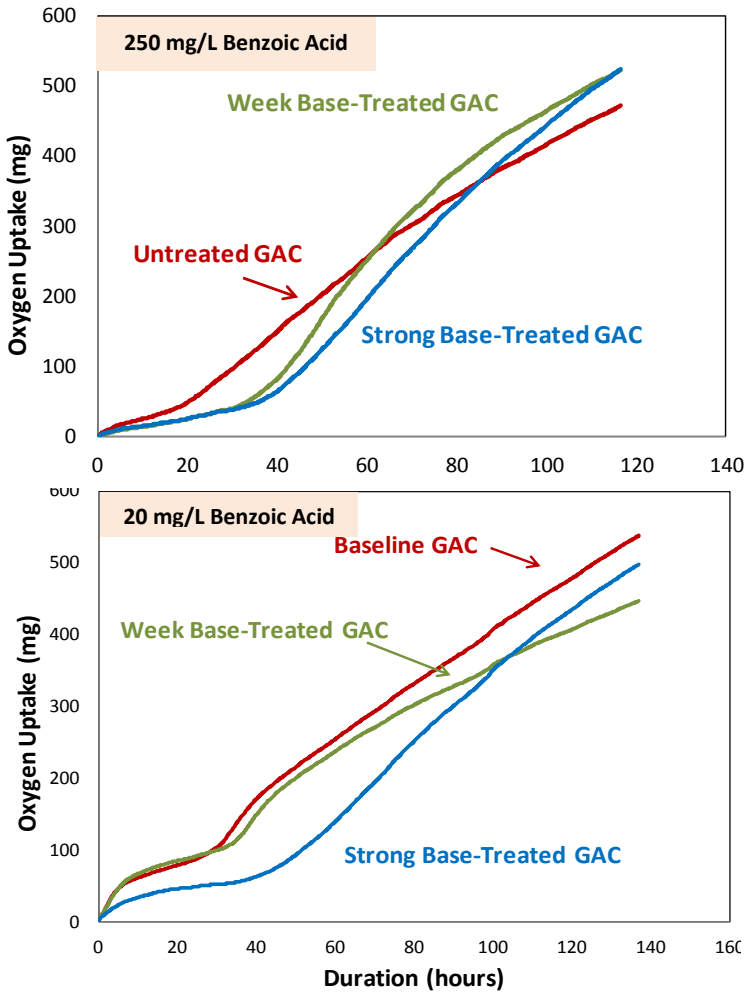

Figure 3.12 - Real-time oxygen uptake volume (mg) of *P. putida* with untreated activated carbon compared to that with the weak base- and strong base-treated activated carbons at 20 ℃. Each reactor was operated at exactly same aqueous concentration of benzoic acid at 250 mg/L and 20 mg/L, respectively. The bacterial growth rate with untreated carbon was significantly higher than that with the two base-treated carbon surfaces at both concentrations of benzoic acid, which is in agreement with our hypothesis. The total oxygen utilization volume of cells with strong base-treated carbon increased after 100 hours due to the low energy production coefficient (f_e), which inhibited the metabolic activity level of bacteria with the strong base-treated GAC.

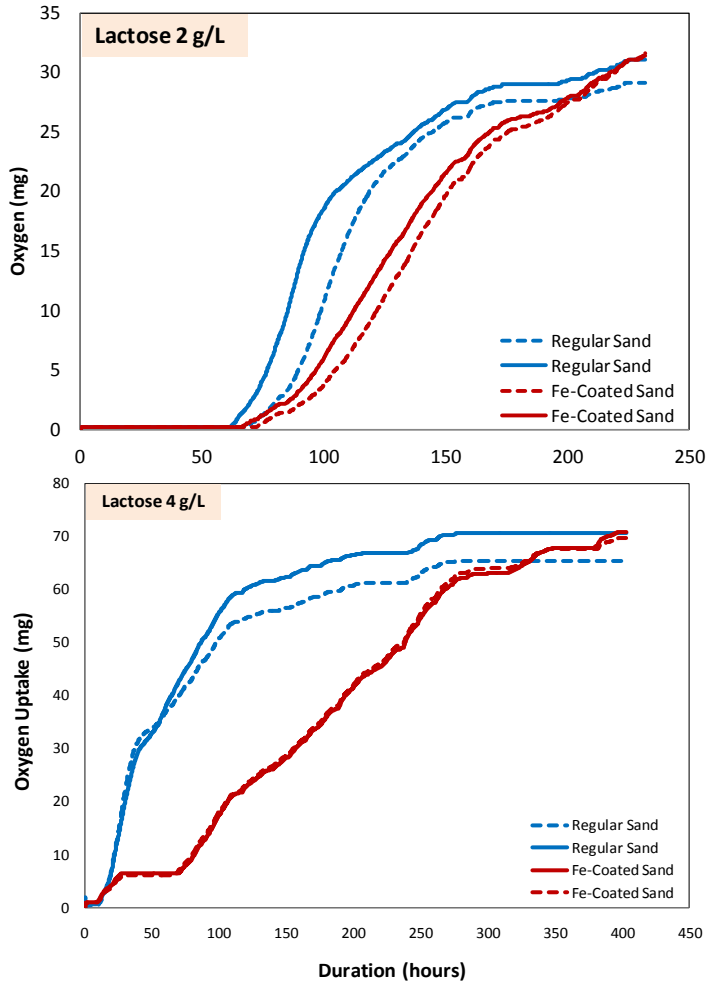

Figure 3.12 - Respirometer results for *P. putida* growing in minimal media with 2 g/L and 4 g/L lactose, respectively. Iron-coated sand exhibited obviously antimicrobial effect on bacterial growth after approximate 70 or 8 hours, which was considered as the 'lag time' prior to that charge-regulated surfaces started obviously affecting on the growth of *P. putida* cells. After the 200- or 300- hour duration with 2 or 4 g/L lactose, the oxygen uptake volume turned to be close due to the huge amount of planktonic cell growth and biofilm formation.

3.4 Conclusions

Both original and surface modified materials were examined to analyze their physicochemical nature in conjunction with aerobic biodegradation, which was represented in terms of oxygen uptake volume. The surface properties were characterized and quantified through our charge-regulation model via dissociation constant (K) and site density (N) of each acidic/basic functional group at the surfaces. Given the values of K and N, the charge-regulation model was able to simulate the electrostatic behavior of cells approaching such negatively/positively charged surfaces and to estimate how the microbial growth varies responding to bacterial adhesion.

Our hypothesis based on a link between the charge-regulation effect and cellular bioenergetics, which is applied here to explore the effect of surfaces with different functional group species (different K values) on the metabolic activities and microbial growth. The results demonstrated that the treated material surfaces with more positive charge (containing more basic functional groups) possessed an antimicrobial nature considering both base treated activated carbon and iron-coated sand. That clearly verified our hypothesis, and provided a way to select appropriate surface treatment in industries depending on specific application.

References

Baker K.H. and Herson D.S. (1994) Bioermediaiton. McGraw-Hill, New York, pp. 1-7.

Benjamin M.M., Sletten S.R., Bailey P.R., and Bennett T. (1996) Sorption and filtration of metals using iron-oxide-coated sand. Water Research. 30(11), 2609-2620.

Boopathy. R. (2000) Factors limiting bioremediation technologies. Bioresource Technology 74(1), 63-67.

Hobbie J.E. , Daley R.J. and S. Jasper. (1977) Use of nuclepore filters for counting bacteria by fluorescence microscopy, Appl. Environ. Microbiol. 33, 1225-1228.

Hong Y. and Brown, D.G. (2006) Cell surface acid-base properties of Escherichia coli and Bacillus brevis and variation as a function of growth phase, nitrogen source and C:N ratio. Colloids Surf. B 50, 112-119.

Hong Y. and Brown, D.G. (2008) Electrostatic behavior of the charge-regulated bacterial cell surface. Langmuir 24, 5003-5009.

Hong Y. and Brown, D.G. (2009) Variation in bacterial ATP level and proton motive force due to adhesion to a solid surface, Appl. Environ. Microbiol. 75, 2346-2353.

Hong Y. and Brown, D.G. (2010) Alteration of bacterial surface electrostatic potential and pH upon adhesion to a solid surface and impacts to cellular bioenergetics, Biotechnol. Bioeng., 105 965-972.

Hong Y. and Brown, D.G. (2011) Impact of the Charge-Regulated Nature of the Bacterial Cell Surface on the Activity of Adhered Cells, J. Adhesion Sci. Technol. 25, 2199-2218.

Jones, D., Pell P.A. and Sneath, P.H.A. Maintenance of bacteria on glass beads at -60℃ to -76℃, in: B.E. Kirsop, A. Doyle (Eds.) Maintenance of microorganisms and cultured cells: A manual of laboratory methods, Academic Press, San Diego, 1991.

Mangun C.L., Benak R.K., Daley A.M., and Economy J. (1999) Oxidation of Activated Carbon Fibers: Effect on Pore Size, Surface Chemistry, and Adsorption Properties. Chem. Mater 11, 3476-3483.

Rijnaarts H.H.M., Norde W, Lyklema J, Zehnder J.B.A. (1996) Colloids and Surfaces B: Biointerfaces. 4(4), 191–197.

Shafeeyan S.M., Wan Mohd Ashri Wan Daud, Houshmand A, Shamiri A. (2010) A review on surface modification of activated carbon for carbon dioxide adsorption. Journal of Analytical and Applied Pyrolysis. 89(2), 143-151.

CHAPTER 4

IMPACT OF THE CHARGE-REGULATION EFFECT ON THE BIOAVAILABILITY OF IONIZABLE ORGANIC SUBSTRATES SORBED ON ACTIVATED CARBON

CHAPTER 4. Impact of the Charge-Regulated Effect on the Bioavailability of Ionizable Organic Substrates Sorbed onto Activated Carbon

4.1 Introduction

There's increasing attention on the removal efficiency of trace organic pollutants from water. While activated carbon may be a feasible option for removal of trace organic pollutants, its use requires treatment or disposal of the spent carbon to minimize environmental impacts. One viable approach is to use biological treatment to degrade the organics that are now concentrated in the activated carbon (Schmidt L.M., *et al*., 1999; Abumaizar J. R., *et al*., 1998), and this has been applied in trickling filters, bio-filters and bio-scrubbers (Dharmavaram S., 1991; Chen *et al*., 1992).

The rate at which bacterial cells can convert contaminants during biodegradation depends on the rate of contaminant uptake and transfer to the cells (Boopathy and Manning, 1998). When considering bioavailability of sorbed substrates, this involves multiple physicochemical process including sorption, desorption and diffusion, and the overall bioavailability is widely considered as the primary limitation in many environmental clean-up remedies. While, past studies indicated that the bioremediation of aqueous organic pollutants could be feasible by combing the physical adsorption process onto effective sorbents, the overall biodegradation rate will be controlled by the rate that the sorbed substrates become available to the bacteria.

Commercial granular activated carbon (GAC) has a high adsorption capability of organic solutes from the aqueous phase and can be applied in batch, column, or fluidized-bed operations. The high sorption capacity of GAC is due to its high surface areas, well-developed internal micro-porosity and the wide spectrum of surface functional groups (Chingombe P. *et al.,* 2005). Combination of biodegradation and sorption onto activated carbon has been shown to work well for the treatment of many organic contaminants (Ehrhardt N.M. and Rehm H.J. 1985; Voice T.C. *et al.,* 1992). This combination results in shorter treatment times, higher removal efficiency, and more environmentally benign products, compared to conventional chemical, physical, or biological systems (Wang S. and Zhu Z.H., 2005).

The bioavailability of sorbed organics is related to the sorption isotherm and desorption kinetics. When considering ionizable substrates, Al-Degs et al. (2007) reported that the solution pH strongly influences their sorption behavior on activated carbon. This is of interest here, as our working hypothesis with the charge-regulation effect is based on local pH changes during bacterial adhesion (Hong Y. and Brown D.G., 2009). Accordingly, we expect the sorption/desorption capability of activated carbons, and thus the bioavailability of ionizable substrates, can be altered during bacterial adhesion, with the effect related to the acid/base properties of the adhering surface.

We performed a thorough literature review, and neither experiment- or modeling- based studies have been conducted that examined pH-controlled desorption of sorbed organic compounds. Thus, it was unclear as to how local pH variations during bacterial adhesion

could affect contaminant bioavailability. To answer this, we performed experiments using both ionizable and nonionizable organic compounds including benzoic acid (a weak acid), benzylamine (a weak base) and ethylbenzene (a neutral compound) and it was expected that these compounds would exhibit different pH-dependent sorption isotherms. Three activated carbons were used, including a commercially-available (untreated) carbon with weak-acid functionality, a surface-modified carbon with weak-base functionality, and a surface-modified carbon with strong-base functionality It was expected that the local pH values were vary from acidic to basic during bacterial adhesion due to the charge-regulation effect. We performed respirometry experiments on the organic biodegradation rate, represented in terms of oxygen uptake, in conjunction with the investigation of sorption capability of organic compound from aqueous solution onto activated carbon. The results demonstrated a link between bacterial adhesion and local charge-regulated pH variations on the sorption capacity and bioavailability of ionizable contaminants.

4.2 Materials and Methods

4.2.1 Bacterial Culture

The gram-negative bacteria strain *Pseudomonas putida* (ATCC 31947) was used in this study. Bacterial cultures were grown at 30℃ in 250 mL of Luria Bertini broth (LB broth, Fisher Scientific). Cells were harvested in the exponential phase, then mixed with

15% glycerol and stored at -86 ℃ using the glass bead method (Y. Hong and D.G. Brown, 2009; Y. Hong and D.G. Brown, 2008; J. Jones, P.A. Pell, *et al*., 1991).

For each experiment, *P. putida* from the frozen stock was cultivated in minimal growth media at 30 ℃ for 36 hours. The minimal media composition includes 5.44 g/L KH_2PO_4, 0.5 g/L NH_4Cl, and 0.6 mL/L inorganic salt stock solution (containing 10 g/L $MgSO_4 \cdot 7H_2O$, 0.1 g $CaCl_2 \cdot 2H_2O$, 0.4 g $FeSO4 \cdot 7H_2O$, 1.0 g $MnCl_2 \cdot 2H_2O$ in 1 L). The pH was adjusted to 7.2 with 3 N NaOH (and/or 1 N HCl). The cells were grown to the late exponential phase and prior to use.

A bacteria washing/starvation process was applied to prepare cells prior to zeta potential measurements. The cells were harvested and washed twice by centrifuging the suspension at 3500 ×g for 15 minutes at room temperature, followed by re-suspending the bacterial cells in phosphate buffer solution (PBS, 0.258g KH_2PO_4 and 0.470g K_2HPO_4 in 1 L DI water with the pH adjusted to 7.2 using 3 N NaOH). The bacteria suspension was then placed on a rotary shaker for a 24-hour starvation period prior to a second time washing and re-suspending in a specific electrolyte solution for the zeta potential measurements. This starvation process was to deplete the microbial energy reserves. The cell suspensions were diluted with the test solution to a concentration of approximately 10^6 cells/mL determined by Acridine Orange direct counts (J.E. Hobbie, R.J. Daley, *et al*., 1977).

4.2.2 Preparation of Solid Surfaces

Three activated carbons were provided by Evoqua Water Technologies, LLC. These include an untreated activated carbon, a surface-modified activated carbon with weak-base functionalities, and a surface-modified activated carbon with strong-base functionalities.

GAC fines were obtained for the zeta potential experiments by crushing the dry granular particles in a mortar, suspending the crushed particles in 50 mL of electrolyte solution and allowing the coarser particles to settle out of solution. The supernatant was used directly for zeta potential analysis with a Zetasizer Nano ZS (Malvern Instruments). Size analysis showed that the resulting fines had a mean effective diameter of 0.37 microns.

For the biodegradation experiments, the activated carbons were ground to US mesh 200x325, followed by wet sieving, washing and dried at 60℃ overnight.

4.2.3 Surface Characterization

The solid surfaces were observed on Scanning Electron Microscope (SEM)/Energy Dispersive X-ray Spectroscopy (EDS). The basic groups used in the surface-modification of both the weak-base and strong-base GACs were nitrogen-based. To verify the presence of the surface groups, the nitrogen element distribution on the carbon surface was determined via surface elemental mapping via EDS analysis.

The electrophoretic mobility/zeta potential profile of both *P. putida* cells and solid surfaces were examined by titrating across the pH range of 2.5-9.5. The zeta potentials of cells and of fine particles obtained from crushing GAC and measured using Malvern Zetasizer Nano ZS in a 10 mM NaCl solution, with the pH adjusted with 0.1 N NaOH and 0.1 N HCl.

4.2.4 Sorption Isotherm Determination

Single-solute isotherm experiments were conducted to determine the adsorption capability of the three substrates at three different pH values (4, 7, 9). GAC particles (0.2 g) were added into sealed glass bottles containing 100 mL phosphate buffer (10.88 g/L KH_2PO_4 with the pH was adjusted by either 3 N NaOH or 3 N NaOH). The target organic compound was added to the bottles in the concentration range of 50 mg/L to 500 mg/L. After a five-day equilibrium period, the GAC particles were removed by sedimentation and filtration through 0.2-μm filters. The supernatant from each bottle was analyzed for the concentration of the target organic using high performance liquid chromatography with diode array detection (HPLC/DAD) for benzoic acid and benzylamine and gas chromatography with flame ionization detection (GC/FID) for ethylbenzene.

4.2.5 Aerobic Respiration Experiment

The microbial biodegradation rate was represented in terms of oxygen uptake using a batch respirometer system with a water bath at 20℃. We used custom-designed

bioreactors (Figure 4.1) that consisted of 1L media bottles with the caps modified to hold two open test tubes containing 1 M NaOH solution to remove CO_2 from the headspace. The caps were also modified with hanging stir bars to allow the GAC to remain completely mixed without grinding at the reactor bottom. The real-time oxygen consumption (expressed as total oxygen uptake volume as a function of time) was measured and recorded automatically by the PF-8000 Aerobic Respirometer System (Respirometer Systems and Applications, LLC). The experiment was initiated by adding 10 ml of *P. putida* suspension into 690 ml minimal media, along with 0.28~0.37 grams of GAC and sufficient organic growth substrate to obtain an initial aqueous concentration of 0.1 mg/L (mass of substrate added to the reactor was determined using the sorption isotherms).

4.2.6 Desorption kinetics determination

The bench-scale system was performed to track dynamic desorption of benzoic acid and benzylamine from activated carbon, and to evaluate the shifting in sorption capability due to pH variation. The GAC particles were equilibrated with solution containing ionizble substrate at neutral pH. Samples were collected over time and analyzed. Upon demonstrating equilibrium, the pH was changed from pH 7 to either pH 4 or 9 by adding 3 N HCl or 3 NaOH, respectively, and samples collection continued until a new equilibrium was demonstrated.

4.3 Results and Discussion

4.3.1 Surface Characterization of Activated Carbons

The surface structure of each carbon (untreated activated carbon, weak base- and strong base-treated activated carbons) was determined on Scanning electron microscope (SEM) and showed in Figure 4.2. Energy Dispersive X-ray Spectroscopy (EDS) analysis determined the element distributions of carbon, oxygen and nitrogen at carbon surfaces. Untreated activated carbon had no detectable nitrogen at the surface. Strong base-treated carbon surface carried nitrogen at a weight ratio of 3.65%, which was higher than that of weak base-treated carbon surface at 1.78%. Oxygen content remained constant on surfaces of untreated and base-treated activated carbon at a weight percentage of 10.0 approximately, which is consistent as previous reports (Mangun *et al*., 1999; Shafeeyan *et al*., 2010). The EDS results indicated that the base treatment add basic functional groups onto the carbon surfaces, which was further verified via surface charge calculation.

The surface charge at GAC surfaces was calculated from zeta potential profile as a function of pH through the charge-regulation model (as described in Chapter 2) via electrophoretic mobility experiment (Figure 4.3). A variation in isoelectric point (IEP) of 3 GACs in Figure 4.3 was observed, shifting from approximately 2.5 for both untreated carbon and weak base treated carbon surfaces to around 4.2 for the strong base treated

carbon surface. The result demonstrated that strong base-treated activated carbon surface carried more basic functional groups exhibiting a positive charge at the surface. This shifting in surface charge among three carbons could be potentially underestimated due to more fresh surfaces exposed to bulk solution resulting from crushing procedure.

Figure 4. 1 - The bioreactor we designed and fabricated in our lab. The caps were modified to hold two tube containers containing 1 M NaOH solution to capture CO_2 produced by metabolic activities. One hanging stir bar was also modified and attached onto each cap to allow all particles to remain completely mixed without grinding at the reactor bottom.

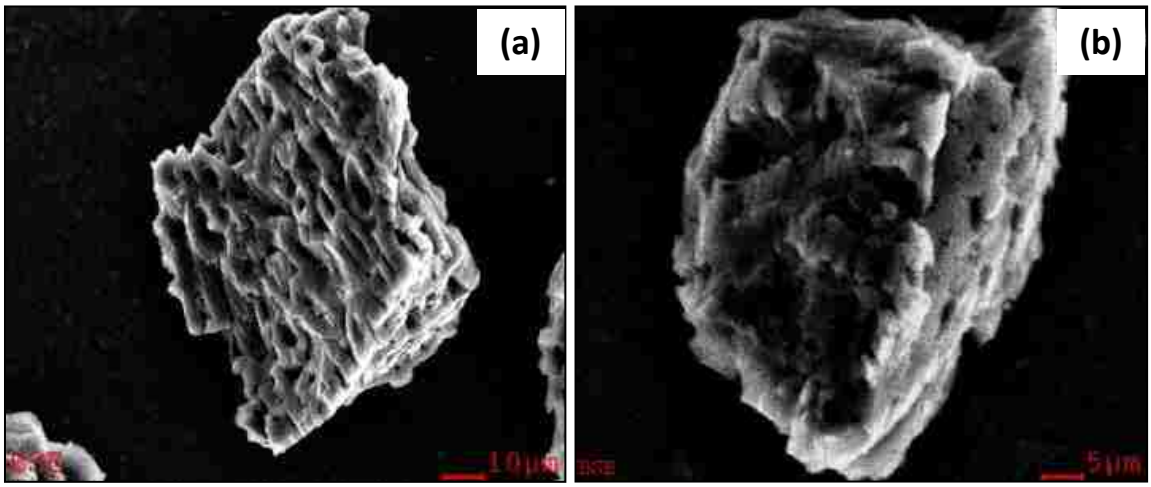

Wt %	Carbon (C)	Oxygen (O)	Nitrogen (N)
Untreated GAC	90.76	9. 24	0. 00
Weak Base-Treated GAC	88.12	10. 10	1. 78
Strong Base-Treated GAC	85. 64	10. 72	3. 65

Figure 4.2 - Scanning electron microscope (SEM) / Energy Dispersive X-ray Spectroscopy (EDS) images of activated carbon particles. (a) Untreated activated carbon; (b) Weak base-treated carbon; (c) Strong base-treated carbon. EDS analysis determined the element distributions of carbon (C) and oxygen (O), respectively. The weight percentage of nitrogen detected at strong base- and weak base-treated carbon surface was 3.65% and 1.78%, respectively. No nitrogen was detected on untreated carbon surface.

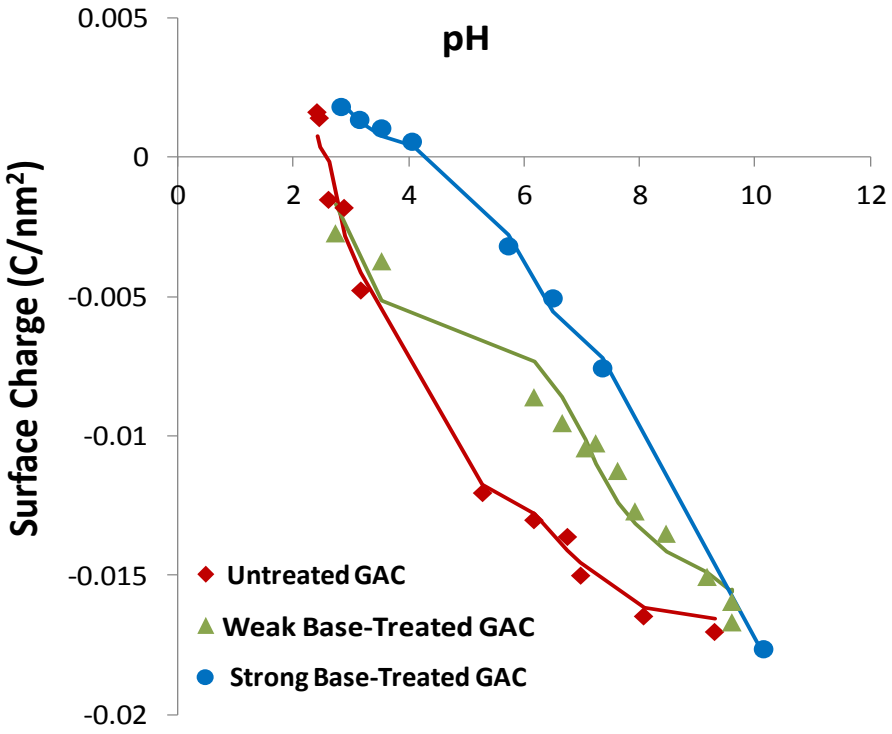

Figure 4.3 - Surface charge of three GACs including untreated GAC, and both weak base- and strong base- treated GAC.

4.3.2 Sorption Isotherm for GACs

The sorption isotherm of selected ionizable substrates (benzoic acid, benzylamine and ethylbenzene) onto untreated and base-treated GACs was determined in a wide pH range of 4 to 7 (Appendix). We observed a high affinity between the sorbent surface (GAC) and the ionizable substrate molecules. The experimental data showed good correlation with the Ferundlich isotherm models.

Figure 4.4 presented the sorption isotherm for benzoic acid sorbed onto untreated GAC for example. The sorption capacity of benzoic acid was higher in acidic bulk than that in basic solution, while, in another way, the adsorption of benzylamine onto all activated carbon was enhanced in basic solution compared to that in acidic solutions (Appendix A.3). No significant variation among three sorption capacity of GACs was observed at the same pH (either pH 4, 7 or 9).

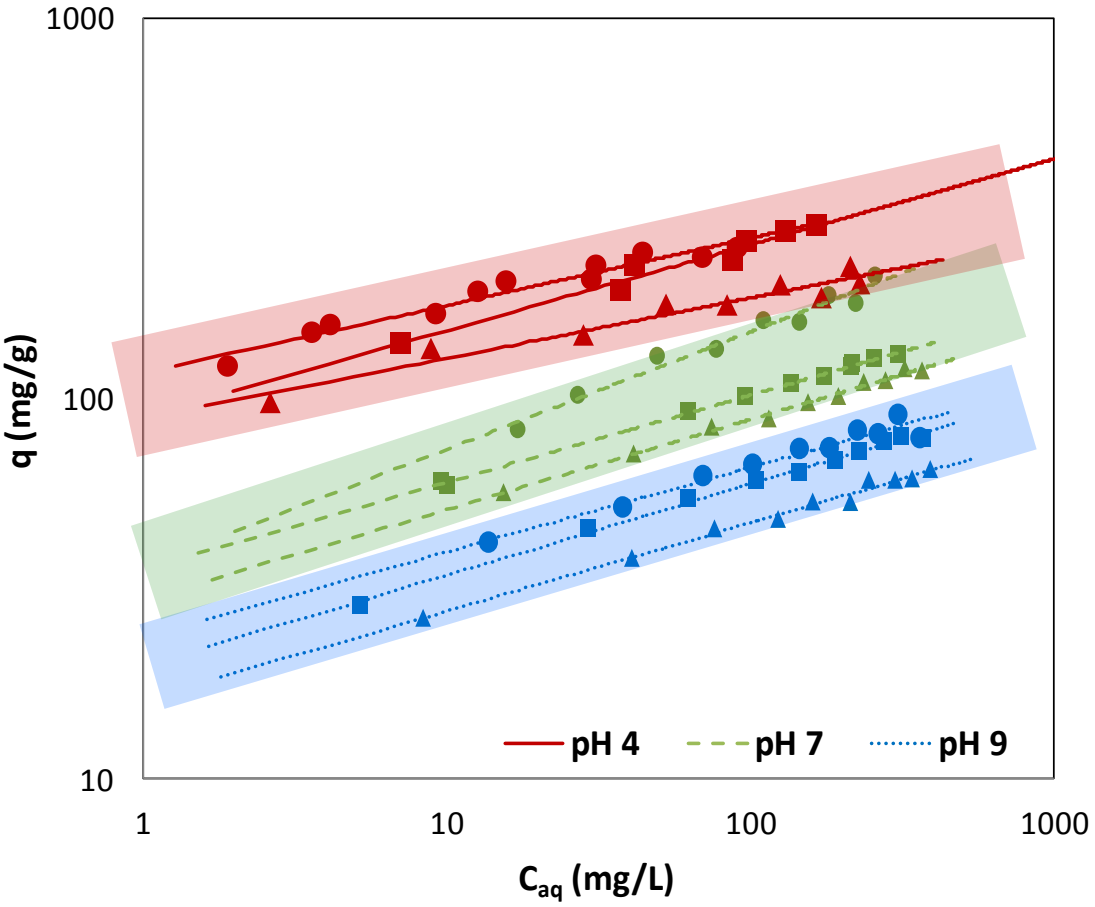

Figure 4.4 - Freundlich fit for equilibrium sorption isotherms of benzoic acid onto untreated GAC, weak base-treated and strong base-treated GACs. All the isotherms are presented in a log-log scale graph. Round symbols (●) are with the untreated GAC and square symbol (■) and triangle symbol (▲) are with weak base- and strong base-treated GACs, respectively. The red, green and blue shading highlight the sorption isotherms at the bulk pH of 4, 7 and 9, respectively.

4.3.3 Oxygen Uptake and Bacterial Growth

Our working hypothesis predicts a variation in surface pH occurs upon bacterial adhesion at both cell surface and GAC surfaces due to charge-regulation effect. The varied surface pH of solids will have a corresponding impact on material sorption capability. The aqueous concentration of the bulk will be altered, which directly affects, if not governs bacterial growth kinetics.

The overall real-time oxygen utilization with benzoic acid for three GACs was shown in Figure 4.5. And Figure 4.5 indicates the bacterial growth for cells with benzylamine. The results demonstrated that under the substrate limit condition (aqueous concentration as low as 0.1 mg/L), the bacterial growth rates with strong base- and weak base-treated GACs were significantly higher than that with untreated carbon within a period of 340 hours after inoculation. Meanwhile, we observed that few planktonic cells were grown in the reactors with untreated GAC; while, a plenty of cells existed with base-treated carbons. This could be explained by the variation in sorption isotherm for each activated carbon.

The results in Section 4.3.2 indicated a substantial reduction in sorption capability for benzoic acid under basic condition (pH 9), and a moderate increase in sorption capability in acidic solution (pH 4). Such variation in sorption isotherm allowed the carbon particles at equilibrium previously to release or sorb ionizable substrate from the bulk, which

influenced the bioavailability of benzoic acid to bacterial cells. When bacteria attached base-treated GAC surfaces containing more positive charge at the surface, the charge-regulation effect induced an increase in surface pH, which resulted in a release of benzoic acid from the equilibrium solid particles to the bulk. The substrate aqueous concentration increased with the isotherm reduction, where the increasing rate depended on desorption kinetics (will talk about it in Section 4.3.4). The bacterial growth represented as oxygen utilization rate was enhanced by the elevated bioavailability of benzoic acid in the reactors. In another way, the bacterial growth with untreated carbon was obviously inhibited by the declined substrate aqueous concentration. The suppressed bioavailability of benzoic acid was induced by decreased surface pH and further enhanced sorption capability of carbon particles upon bacterial adhesion. On the other hand, benzylamine of basic functionality also follows this hypothesis, and the results are described in Figure 4.6.

Since no obvious variation in sorption capacity of ethylbenzene occured at different bulk pH (Appendix A.4), the bioavailability would not change due to surface pH shifting when bacterial cells approach. The respiration experiment for ethylbenzene was also conducted to examine the substrates with neutral functionality and its results are presented in Figure 4.7. Strong base-treated GAC significantly inhibited bacterial growth producing a low level of oxygen utilization, which supports our previous working hypothesis of charge-regulation effect about cellular bioenergetics (talked in Chapter 3). The increased surface pH of cells ultimately declined bacterial metabolic activity levels.

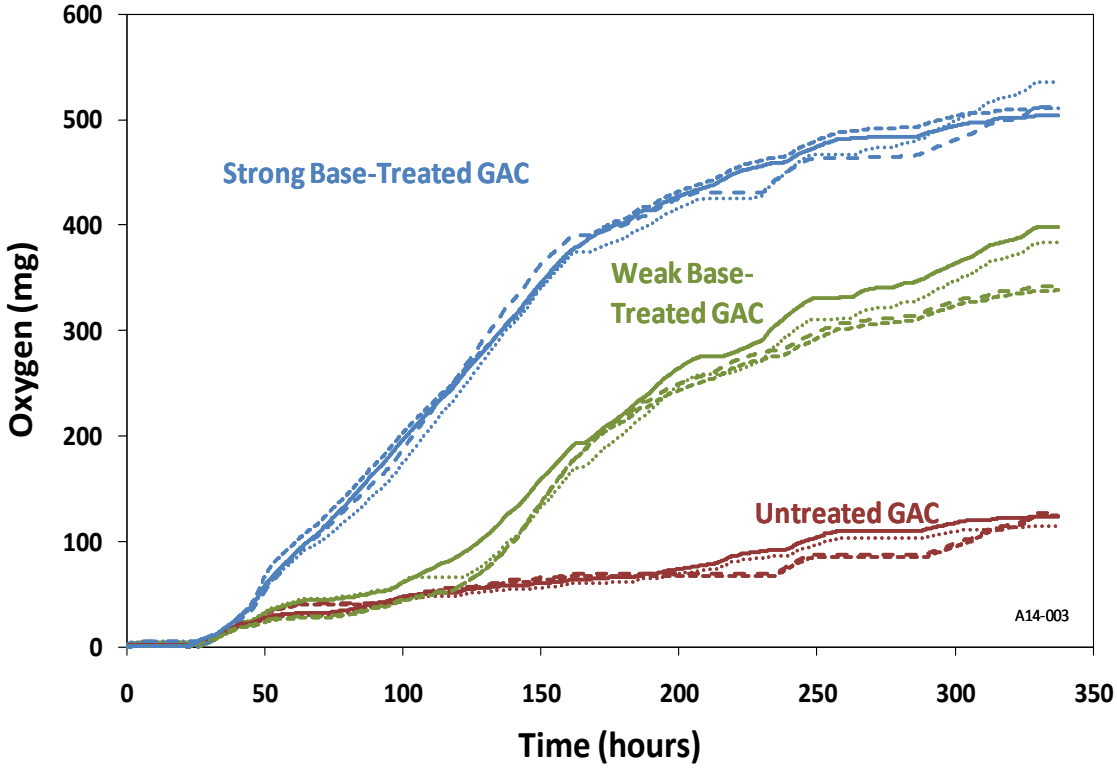

Figure 4.5 - Real-time oxygen uptake volumes from respirometer system for *P. putida* with untreated, weak base- and strong base-treated GACs, where benzoic acid was selected as the sole carbon and energy source. The sorption isotherm (in Section 4.3.2) was prepared to keep the same aqueous concentration of 0.1 mg/L for all reactors. Each line indicates one separate run. The growth rates of bacteria with GACs can be represented in terms of oxygen uptake volumes. Here, bacteria with base-treated GAC exhibited an enhanced growth, which can be well explained through our charge-regulation hypothesis about substrate bioavailability.

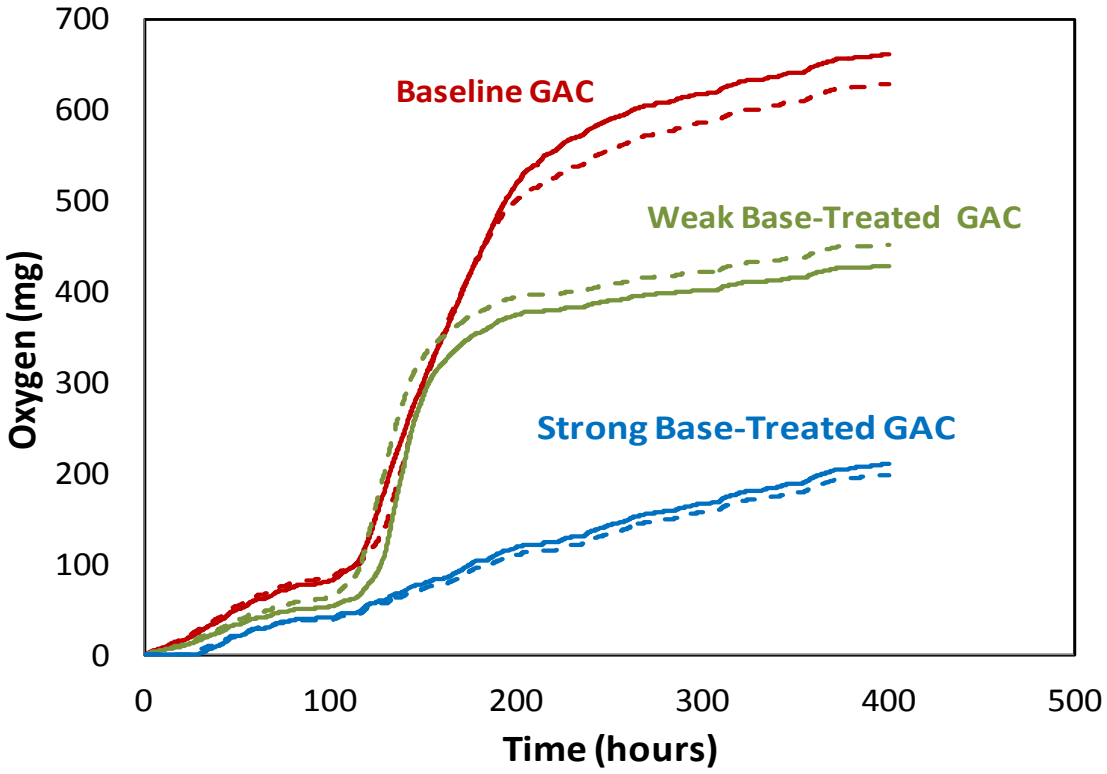

Figure 4.6 - Real-time oxygen uptake volumes from respirometer system for *P. putida* with untreated, weak base- and strong base-treated GACs, where benzylamine was selected as the sole carbon and energy source. Bacterial cells with base-treated GAC exhibited an inhibited growth, which can be well explained through our charge-regulation hypothesis about substrate bioavailability.

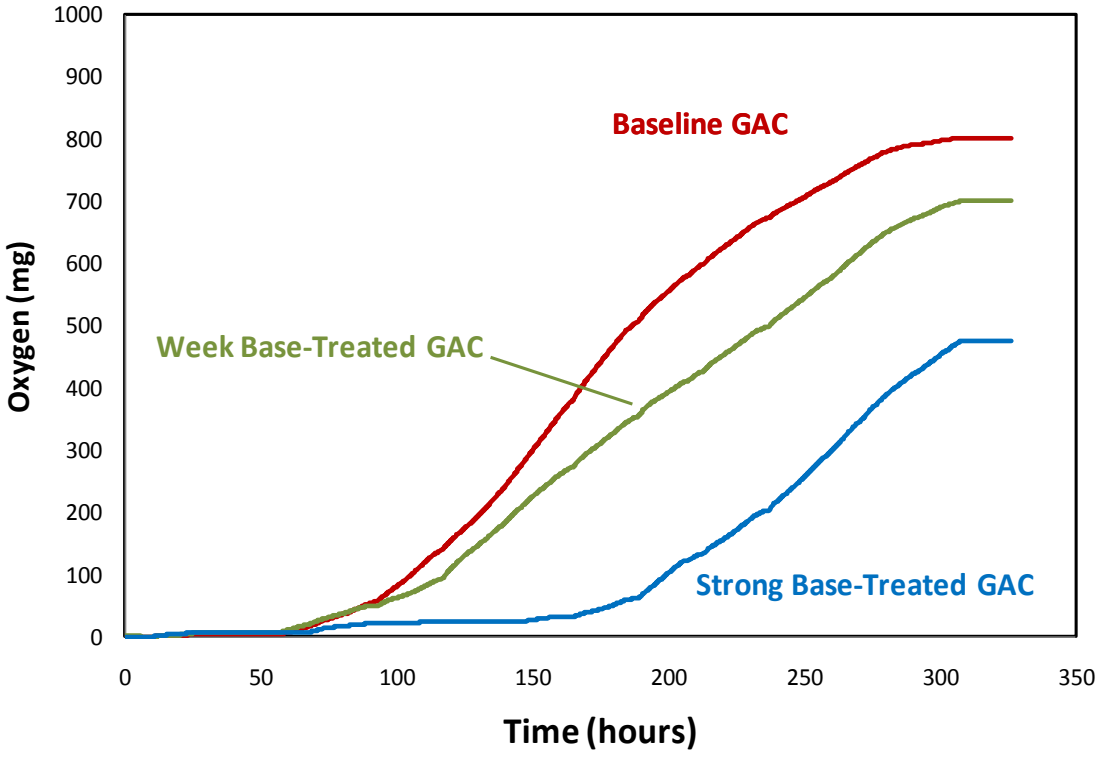

Figure 4.7 - Real-time oxygen uptake volumes from respirometer system for *P. putida* with untreated, weak base- and strong base-treated GACs, where ethylbenzene was selected as the sole carbon and energy source. In this test, the substrate, ethylbenzene is a neutral nonionic compound, and its sorption isotherms at different pH were similar (Appendix). Thus the antimicrobial effect of base-treated GAC follows our charge-regulation hypothesis about celluar bioenergetics via shifting surface pH.

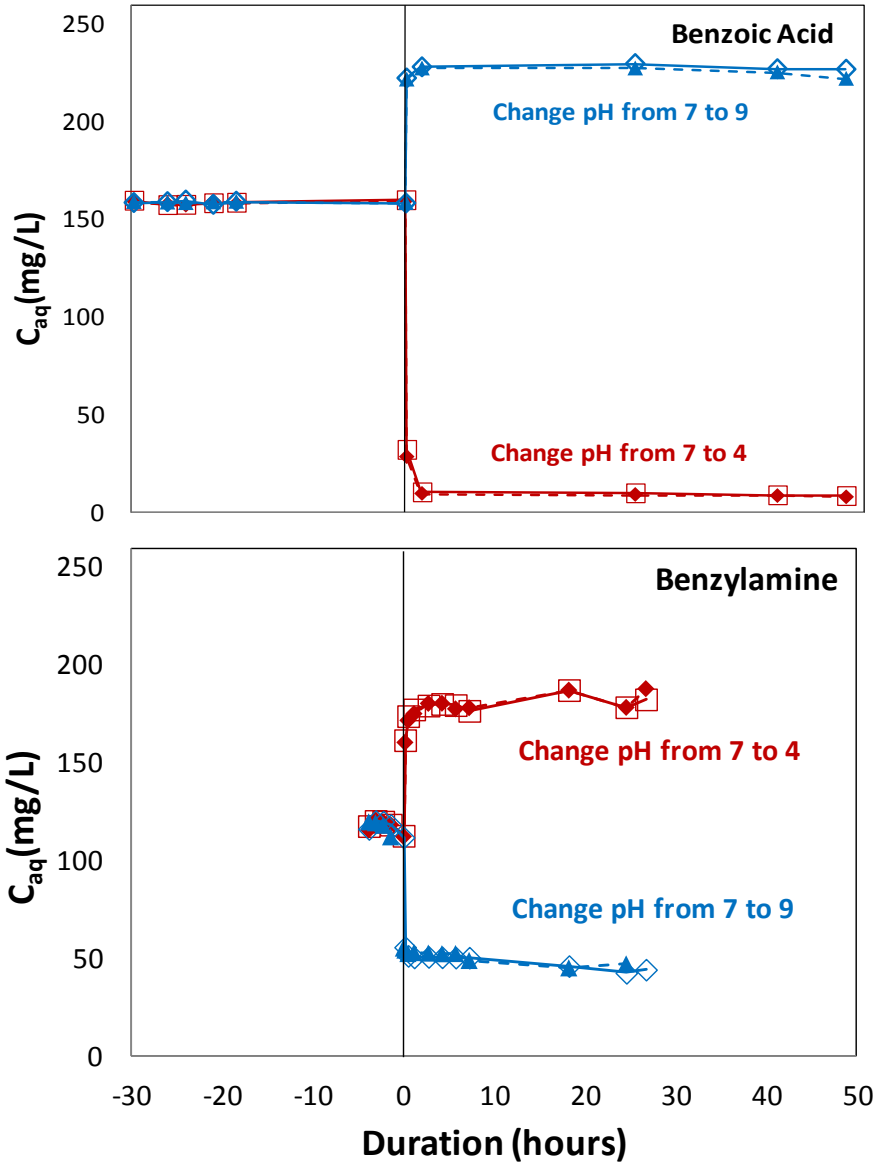

Figure 4. 8 - The variation in equilibrium concentrations of ionizable substrates (benzoic acid and benzylamine) with untreated GAC by altering the bulk pH from neutral to either pH 4 or 9. The desorption kinetics of substrates on GAC is very fast and achieved equilibrium within 15 minutes. The kinetics for the base-treated GACs is similar.

4.3.4 Desorption Kinetics

The material desorption kinetics are vital in governing the dynamic aqueous concentrations of ionizable substrates due to the significant shift in sorption capacity. We examined desorption kinetics of GACs with pH shifting from neutral to either acidic or basic bulk solution (Figure 4.8). The results indicated that the solution was initially equilibrium at neutral pH. When the bulk pH was once increased to 9.0 or decreased to 4.0, approximately, the aqueous concentration got equilibrium within 15 minutes. The fast desorption kinetics allowed the bacterial growth to be directly affected by surface pH and the inducing change in sorption capacity upon cell attachment.

4.4 Conclusions

When substrate is limited, the bioavailability of ionizable substrates could be the dominating aspect in affecting the microbial growth rate. During bacterial adhesion, the local pH between the bacterial and adhering surfaces can change due to the charge-regulation effect. The pH can both increase and decrease from that of the bulk solution, depending on the acid/base functional groups present on the two surfaces. In this study besides bacterial cell surface we demonstrate the charge-regulation effect on solid surfaces on the bioavailability of ionizable growth substrates on surface-modified granular activated carbon (GAC). We examined three different growth substrates –

benzoic acid, ethylbenzene, and benzylamine – which exhibit acid, neutral, and basic functionalities, respectively. Using these growth substrates, we examined their sorption and bioavailability with three GACs, including the untreated carbon and the weak base-treated and strong-base treated carbon. Zeta potential analysis showed that the untreated carbon surface was acidic in nature while the treated carbons contained basic functional groups. Substrate sorption on the GACs was a strong function of pH (Figure 4.4) and this directly affected the bioavailability of the different growth substrates on the three different GACs, and accordingly influenced bacterial growth.

We demonstrate through experimental and numerical results how the charge-regulation effect induces changes in local pH, which in turn alters the bioavailability of sorbed ionizable growth substrates. In addition, the experiment on neutral substrate (ethylbenzene) indicated that positively-charged GACs presented antimicrobial properties, in agreement with our working hypothesis for charge-regulated surfaces. Overall, these findings have implications for the bioavailability of ionizable substrates at surfaces, whether sorbed or in solid form, and understanding of this effect can lead to more effective selection and design of absorbents for specific application.

References

Abumaizar J.R., Kocher W., Smith H.D. (1998) Biofiltration of BTEX contaminated air streams using compost-activated carbon filter media. Journal of Hazardous Materials 60, 111-126.

Al-Degs S.Y., El-Barghouthi I. M.,El-Sheikh H.A., *et al*. (2008) Effect of solution pH, ionic strength, and temperature on adsorption behavior of reactive dyes on activated carbon. Dyes and Pigments 77, 16-23.

Boopathy R. and Manning J. (1998) A laboratory study of the bioremediation of 2,4,6-trinitrotoluene-contaminated soil suing aerobic anaerobic soil slurry reactor. Water Environ. Res. 70, 80-86.

Chen, Y.M., Abriola, L.M., Alvarez P.J.J. Anid P.J., and Vogel, T.M. (1992). Biodegradation and transport of benzene and toluene in sandy aquifer material: model-experiment comparisons. Water Resources Research 28, 1833-1847.

Chingombe P., Saha B., Wakeman R.J. (2005) Surface modification and characterization of a coal-based activated carbon. Carbon 43, 3132-3143.

Dharmavaram S. Biofiltration: a lean emission abatement technology, Air Waste Manage. Assoc., 84th Annu. Meeting and Exhibition, Vancouver, British Columbia, June 16-21, 1991, pp. 1–16.

Ehrhardt N.M., Rehm H.J., (1985) Phenol degradation by microorganisms adsorbed on activated carbon, Appl. Microbiol. Biotechnol 21,32-36.

Schmidt L.M, Delfino J.J., Preston JF, St Laurent G. (1999) Biodegradation of low aqueous concentration pentachlorophenol (PCP) contaminated groundwater. Chemosphere 38(12), 2897-912.

Voice T.C., Pak D., Zhao X., Hickey R.F. (1992) Biological activated carbon in fluidized bed reactors for the treatment of groundwater contaminated with volatile aromatic hydrocarbons. Water Res. 26(10), 1389-1401.

Wanga, S, Zhua Z.H., Coomesb A., Haghsereshtc F., Lu G.Q. (2005) The physical and surface chemical characteristics of activated carbons and the adsorption of methylene blue from wastewater. Journal of Colloid and Interface Science 284 (2), 440-446.

Wang S and Zhu. Z.H. (2007) Effects of acidic treatment of activated carbons on dye adsorption. Dyes and Pigments 75(2), 306-314.

CHAPTER 5

SUMMARY AND CONCLUSIONS

CHAPTER 5 Summary and Conclusions

5.1 Summary

Our study demonstrated the effects of the charge-regulation process on both cellular bioenergetics, with a focus on actively-growing bacteria, and sorption of ionizable growth substrates, with a focus on the impact on substrate bioavailability. Our hypothesis is based on a link between the charge-regulation effect and cellular bioenergetics, which is applied here to explore the effect of surfaces with different functional groups (different K values) on the metabolic activities and microbial growth. During bacterial adhesion, the local pH between the bacterial and adhering surfaces can change due to the charge-regulation effect. The pH can both increase and decrease from that of the bulk solution, depending on the acid/base functional groups present on the two surfaces. Here we analyzed the physcochemical properties in conjunction with aerobic biological process to verify a link between the surface functional groups, aerobic microbial growth, and bioavailability of ionizable growth substrates.

Both original and surface modified materials were used in biodegradation tests, and the result was represented in terms of oxygen uptake volume. The charge-regulated surfaces were characterized for the dissociation constants (K) and site densities (N) that best represent the surface charge density and electrostatic potential. The resulting values of K and N were used with the charge-regulation model to simulate the electrostatic behavior

of cells approaching negatively- and positively-charged surfaces, allowing estimation of how growth of attached bacteria would be affected.

This study provides an understanding about the biological implications of charge-regulated changes in local pH, which in turn alters both cellular bioenergetics and bioavailability of sorbed ionizable growth substrates. Overall, these findings provide insight into the effective selection and design of surfaces and growth substrates given the goals of the system at hand.

5.2 Specific Findings

5.2.1 A simple method was developed to characterize the functional group dissociation constants and site densities that best-represents a charge-regulated surface.

A mathematic approach was developed for quantifying the functional group dissociation constants (K) and site densities (N) that best represent a given charge-regulated surface in an aqueous system. This approach requires zeta potential-pH titration data, along with the specific electrolyte concentrations at each data point. This data is easily obtained using electrophoretic mobility expermients (for colloidal particles) or streaming potential experiments (for granular and planar materials). This approach was demonstrated here using the untreated GAC and it was then applied to all materials used in the study. Most

notably, the approach developed here does not require a fixed ionic strenth, and in fact, more robust results are obtained using data at different ionic strengths.

5.2.2 The charge-regulation effect alters bacterial growth in agreement with the working hypothesis.

Both sand (regular and iron-coated sands) and activated carbon (untreated GAC and GAC given weak and strong base surface functionalities) were selected as solid surfaces in this study. Surface characterization demonstrated that the untreated sand and GAC both had acidic functionalities while the surface-treated sand and GACs contained basic functional groups. Thus following our working hypothesis, it was expected that the treated materials would result in slow growth rates than the untreated materials. Additionally, biological stoichiometric modeling indicated that the treated surfaces would result in a higher overall O_2 utilization due to the redirection of cellular function to energy generation. These effects were observed for respirometer experiments for the sands and GACs, supporting the working hypothesis and indicating that appropriate selection of materials can be used to manipulate growth of attached bacteria.

5.2.3 The charge-regulation effect alters sorption, and thus bioavailability, of ionizable growth substrates.

When two charged surfaces approach each other, such as a bacterium approaching a solid surface, the local pH between the two surfaces will change. We demonstrated that this

local pH change can have a significant effect on the sorption of ionizable substrates onto activated carbon Most notably was when the sorbed substrate's sorption was decreased, releasing the substrate into solution and making it available to the bacteria in the reactor. Using weak acid (benzoic acid), weak base (benzylamine) and uncharged (ethylbenzene) growth substrates, we demonstrated that the sorption and resulting bioavailability directly follows that predicted by the charge-regulation effect. The elucidation of this process in this study provides insight into the selection of surface and growth substrate properties to enhance or inhibit bacterial growth by controlling substrate bioavailability.

5.3 Recommendations for Future Work

The results presented above demonstrate that the charge-regulation effect directly affects microbial growth and bioavailability of sorbed ionizable substrates. These results open up potential future avenues of research, identified below.

5.3.1 Examination of a broader selection of materials for their effects on bacterial growth kinetics.

The study performed here was the first to examine bacterial growth in the context of cellular bioenergetics and the charge-regulation effect. The results followed those predicted by the hypothesis. Future work should focus on determining Monod kinetic parameters for attached bacteria and linking them to biological stoichiometry and cellular bioenergetics. The use of surfaces, such as ion-exchange resins containing specific

functional groups, and additional measurement techniques in addition to respirometry may allow determination of kinetic coefficients of surface-bound bacteria (it should be pointed out that this would not be a trivial undertaking).

5.3.2 Extension of the surface characterization method to bacterial cells.

We developed a quick approach focusing on solid surfaces, which characterized charge-regulated surfaces from zeta potential titration experiments as discussed in Chapter 2. The bacterial surface is not well-defined, as it is composed of surface polymers, proteins and lipids. This outer layer of the bacterial cell is penetrable to ions and water flow, and its analysis is not as straightforward and the concept of zeta potential is not strictly applicable to bacteria. The approach used to interpret electrophoretic mobility of bacteria and other "soft particles" is to titrating as a function of ionic strength and to apply the data to the Naiver-Stokes equation, incorporating fixed charges along the surface polymers. Future work here is to replace the fixed charges with ionizable functional groups and to determine a numerical method for characterizing these surfaces using electrophoretic mobility data as a function of both pH and ionic strength.

5.3.3 Isolation of attached bacterial growth using GAC columns

In this study, we designed the bioreactor for respirometer system to determine bacterial growth in a batch reactor using suspended GAC particles. The batch experiment provided real-time oxygen utilization with the interval as short as 10 minutes, and allowed the

readily controlling over the substrate consumption. However, we also observed planktonic growth in the reactors. One approach to minimize the growth of planktonic bacteria is to use the same three GACs packed into column reactors. The attached bacterial cells would remain in the columns while the planktonic cells would be washed out.

Appendix

SORPTION ISOTHERM OF IONIZABLE SUBSTRATES ON ACTIVATED CARBONS

Appendix: Sorption Isotherm Determination of Ionizable Substrates on Activated Carbons

Single-solute isotherm experiments were conducted to determine the adsorption isotherm of each substrate at the bulk pH of 4, 7 and 9. Selected ionizable substrates included benzoic acid and benzylamine with acidic and basic functionality, respectively, were examined to compare with that with the nonionic compound, ethylbenzene of neutral functionality.

0.2 g GAC (either strong base-, weak base-treated GACs or untreated GAC) particles were added into each sealed bottles containing 100 mL phosphate buffer (10.88 g/L KH_2PO_4; pH was adjusted using either 3 N NaOH or 3 N NaOH). The buffer was used to minimize the shift in bulk pH upon sorption occurs on carbon, and the pH variation was less than 0.6 pH. The aqueous concentration at equilibrium was spread over a range of 10 and 350 mg/L, and the equilibration duration was 5 days with continuously gentle shaking. The remaining aqueous benzoic acid and benzylamine were analyzed on high performance liquid chromatography (HPLC) and the ethylbenzene in bulk was evaluated using gas chromatography (GC).

Freundlich sorption isotherm is commonly used to describe the adsorption characteristics for the heterogeneous surface (Hutson and Tang, 2000). The empirical equation proposed by Freundlich is:

$$Q_e = KC_e^{\frac{1}{n}} \quad (1)$$

Where Q_e is the amount of substrate sorbed per gram of the adsorbent at equilibrium (mg/g), K is Freunlich isotherm constant (mg/g), C_e is the equilibrium concentration of adsorbate (mg/L), n is sorption intensity. By linearizing Equation (1) could be developed as:

$$\log Q_e = \log K + \frac{1}{n}\log C_e \quad (2)$$

The constant K is considered as an approximate parameter indicating sorption capacity, while $\frac{1}{n}$ is a function of sorption strength. Both parameters are typically determined by fitting data to isotherm model.

In this study, preliminary experiment indicated that Freundlich allowed best fit for equilibrium sorption isotherm for all substrates onto GACs. Take the results of sorption isotherms of benzoic acid onto untreated GAC for example (Figure A.1). Figure A.1 (a, b and c) showed how the experiment data fit Freundlich model in normal (analog) scale at the pH of 4, 7and 9. All the data of the three isotherms was combined in Figure A.1 (d) and linearized in log-log scale. The isotherms were visually simplified using a log-log scale and easy to calculate the parameters for Freundlich model. The following Appendix

a, b and c will demonstrate all the sorption isotherms of benzoic acid, benzylamine and ethylbenzene on the three GACs, respectively.

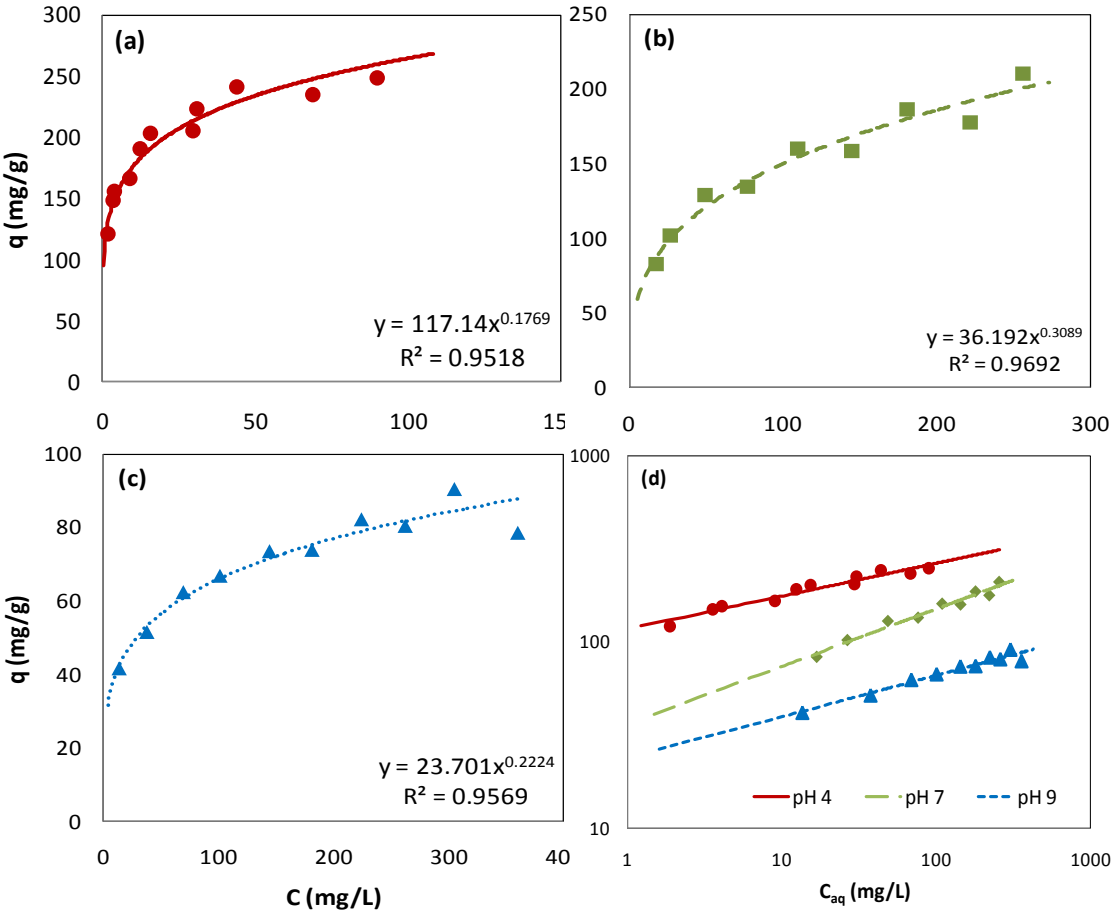

Figure A.1 - Freundlich fit for equilibrium sorption isotherms of benzoic acid onto untreated activated carbon. Figure (a), (b) and (c) showed the sorption isotherm in normal scale at the bulk pH of 4, 7 and 9, respectively; and the overall isotherm are presented in a log-log scale graph (d). The result indicates the sorption of GAC varies under different pH conditions. Round symbols (●) are with the untreated GAC; square symbol (■) and triangle symbol (▲) are with weak base- and strong base-treated GACs, respectively. The red, green and blue shading highlight the sorption isotherms at the bulk pH of 4, 7 and 9, respectively.

Appendix (a): Sorption Isotherm of Benzoic Acid on GACs at pH 4, 7 and 9.

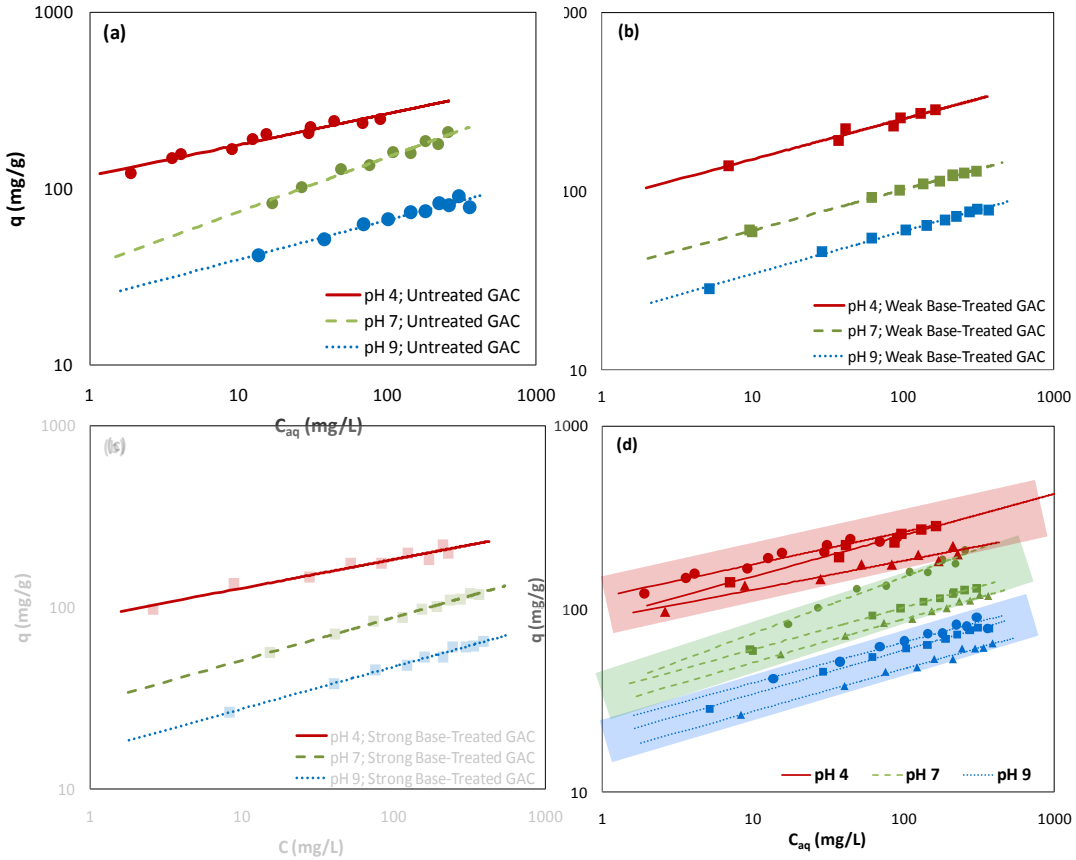

Figure A.2 - Substrate adsorption isotherm of benzoic acid on granular activated carbons (GACs) at pH 4, 7 and 9. GACs include (a) untreated GAC, (b) weak base-treated GAC, and (c) strong base-treated GAC. The overall isotherms of benzoic acid on three GACs are presented in (d). All the isotherms are presented in a log-log scale graph.

Appendix (b): Sorption Isotherm of Benzylamine on GACs at pH 4, 7 and 9.

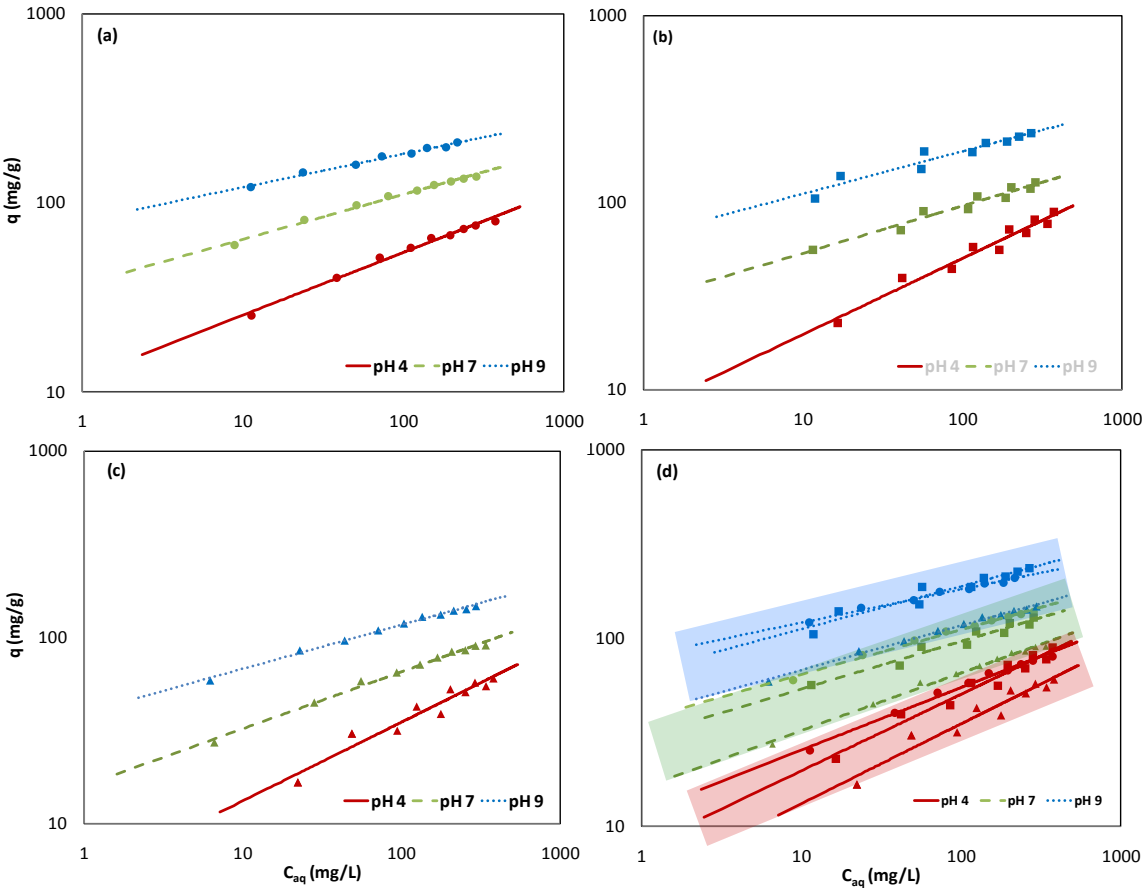

Figure A.3 - Substrate adsorption isotherm of benzylamine on granular activated carbons (GACs) at pH 4, 7 and 9. GACs include (a) untreated GAC, (b) weak base-treated GAC, and (c) strong base-treated activated carbon. The overall isotherms of benzylamine on three GACs are presented in (d). All the isotherms are presented in a log-log scale graph.

Appendix (c): Sorption Isotherm of Ethlybenzene on GACs at pH 4, 7 and 9.

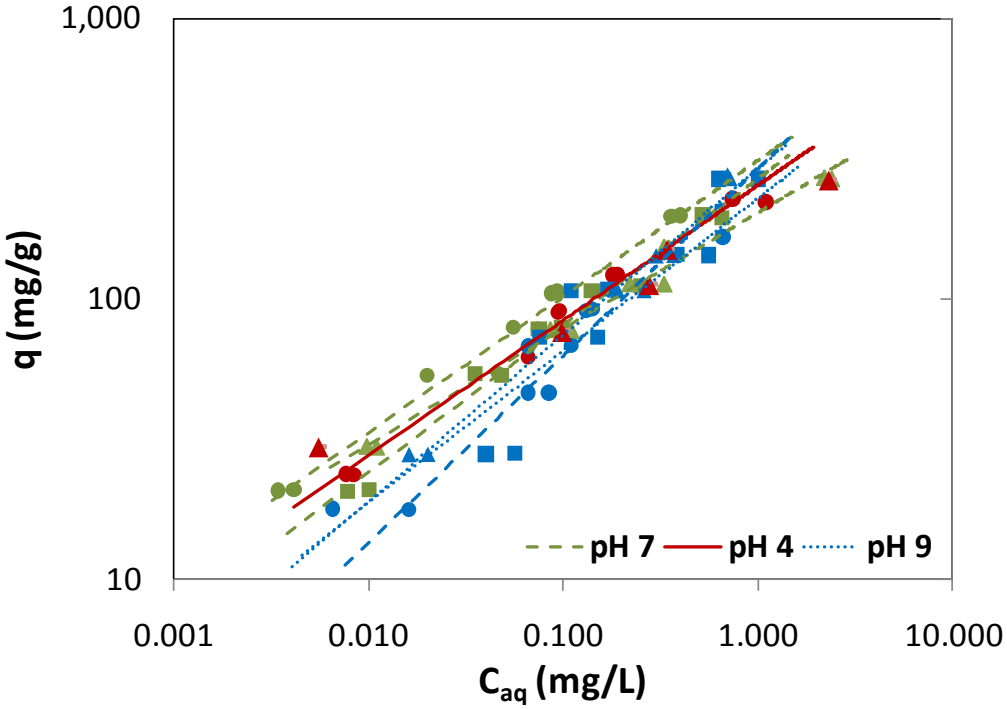

Figure A.4 – Overall substrate adsorption isotherm of ethylbenzene on three granular activated carbons (GACs) at pH 4, 7 and 9. GACs include untreated GAC, weak base-treated GAC, and strong base-treated GAC. All the isotherms are presented in a log-log scale graph. The sorption capacity of ethylbenzene with neutral functionality was not obviously affected by varying pH.

References

Hutson N. D. and Yang. R. T. (2000) Structural Effects on the Adsorption of Atmospheric Gases in Mixed Ag,Li -X Zeolite. AIChE J. 46, 2305.

VITA

Hankai Zhu was born on December 26, 1985, Henan province in China. She received her Bachelor degree of Environmental Science from Nanjing University, Nanjing, China in 2006. She obtained her Master degree of Environmental Science from Nanjing University, Shanghai, China in 2009. She started research towards this doctoral dissertation at Lehigh University in June 2009.